J. Math. Biol. 42, 291–326 (2001)
Digital Object Identifier (DOI):
10.1007/s002850000058

Mathematical Biology

Pietro-Luciano Buono · Martin Golubitsky

Models of central pattern generators for quadruped locomotion

I. Primary gaits

Received: 2 July 1999 / Revised version: 20 March 2000 /
Published online: 16 March 2001 –

Abstract. In this paper we continue the analysis of a network of symmetrically coupled cells modeling central pattern generators for quadruped locomotion proposed by Golubitsky, Stewart, Buono, and Collins. By a cell we mean a system of ordinary differential equations and by a coupled cell system we mean a network of identical cells with coupling terms. We have three main results in this paper. First, we show that the proposed network is the simplest one modeling the common quadruped gaits of walk, trot, and pace. In doing so we prove a general theorem classifying spatio-temporal symmetries of periodic solutions to equivariant systems of differential equations. We also specialize this theorem to coupled cell systems. Second, this paper focuses on *primary gaits*; that is, gaits that are modeled by output signals from the central pattern generator where each cell emits the same waveform along with exact phase shifts between cells. Our previous work showed that the network is capable of producing six primary gaits. Here, we show that under mild assumptions on the cells and the coupling of the network, primary gaits can be produced from Hopf bifurcation by varying only coupling strengths of the network. Third, we discuss the stability of primary gaits and exhibit these solutions by performing numerical simulations using the dimensionless Morris-Lecar equations for the cell dynamics.

1. Introduction

Quadrupedal gaits have been studied by many authors [23, 21, 22, 18, 1, 13, 19, 2] and models of central pattern generators (CPGs) for quadruped locomotion have been studied using a variety of approaches including: equivariant bifurcation theory [9], numerical simulations [7, 10], phase response curves [6], and numerical simulations of an externally aroused CPG [32]. In this paper we continue the study of a CPG model for quadruped locomotion based on symmetry introduced in Golubitsky *et al.* [15].

P.-L. Buono: Centre de Recherche Mathématique, Université de Montréal, C.P. 6128, Succursale Centre-Ville, Montréal, (Qué) H3C 3J7, Canada. e-mail: buono@crm.umontreal.ca

M. Golubitsky: Department of Mathematics, University of Houston, Houston, TX 77204-3476, USA. e-mail: mg@uh.edu

Key words or phrases: Gaits – Symmetry Coupled oscillators – Periodic solutions – Central pattern generators

1.1. Coupled cell systems

One of the early attempts at modeling animal locomotor CPG using coupled cell systems reduced to phase models is due to Cohen *et al.* [8,33] in the case of the lamprey. In this context *cell* means a system of ordinary differential equations. Ermentrout and Kopell [11] have also successfully used coupled cell systems reduced to phase models to describe animal locomotion. Indeed, some of the most significant work on the modeling of CPGs comes from a collection of papers by Kopell and Ermentrout [24–27] where they investigate coupled cell systems as models for lamprey and fish CPGs. In Kopell *et al.* [28], predictions about the lamprey CPG model are made and these predictions are verified experimentally in Williams *et al.* [36].

1.2. Symmetry

The idea of symmetry was introduced into the description of quadruped gaits by Howell [23] and Hildebrand [21]. Schöner *et al.* [35] study the rhythmic patterns of gaits using phase models with symmetry. Collins and Stewart [9] were the first to emphasize symmetrically coupled cell systems as CPG models of quadruped locomotion.

To carry out the modeling, Collins and Stewart [9] make the assumption that the rhythmic gaits of animals mirror the output signals from the CPG. Studies made on primitive vertebrates support this assumption. Indeed, Grillner *et al.* [20] state: "The lamprey spinal cord *in vitro* can produce a motor pattern with a similar phase lag, burst, and cycle duration as the spinal and intact lamprey swimming in a swim-mill" and further on "the same results have been obtained in the spinal dogfish, the decerebrate stingray and the frog embryo". Assuming that symmetric gait patterns mirror the activity of the CPG, it follows that the output signals from the CPG must be symmetric. Thus, as in [9] and [15], we assume that the CPGs possess symmetry.

1.3. The eight-cell network

The CPG model for quadruped locomotion in [15] is a network of identical symmetrically coupled cells. As shown in [15] this network is capable of producing periodic solutions modeling quadruped gaits called *primary gaits*; that is, gaits modeled by output signals from the CPG where each cell emits the same waveform along with exact phase shifts between cells. The primary gaits produced by our model are walk, trot, pace, bound, jump, and pronk. Our contribution to the theory of this CPG model is twofold. First, we show that the proposed quadruped network is the smallest one under the assumptions used to create the model. See Theorem 3.2. Second, under mild assumptions on the cell dynamics and the coupling of the network, we show that by varying only coupling strengths between cells, the network can produce all primary gaits, except pronk, by Hopf bifurcation. See Theorem 4.1.

The proposed coupled cell model consists of eight cells and has the mathematical form:

$$\dot{u}_i = F(u_i) + \sum_{j \to i} \alpha_{ji} H(u_j, u_i)$$

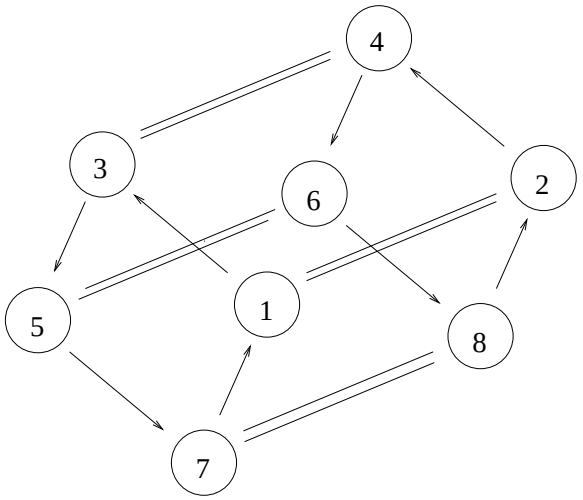

Fig. 1. Schematic eight-cell network for gaits in four-legged animals.

where $u_i \in \mathbf{R}^k$ are the state variables of cell i, the vector field $F : \mathbf{R}^k \to \mathbf{R}^k$ models the internal dynamics of each cell, the function $H : \mathbf{R}^k \times \mathbf{R}^k \to \mathbf{R}^k$ models the coupling of one cell to another, and α_{ji} is the strength of coupling from cell j to cell i. Observe that the sum is taken only over those cells j that are actually coupled to cell i. The network in [15] has the form of two unidirectionally coupled rings of four cells, as shown in Figure 1. In that model the output u_1 is sent to the left hind leg; output u_2 is sent to the right hind leg; output u_3 is sent to the left fore leg; and output u_4 is sent to the right fore leg.

Some of the gaits commonly used by quadrupeds are the walk, trot, pace, bound, transverse gallop, rotary gallop, and canter. For example, in a walk, each leg strikes the ground in turn in a figure eight pattern with a quarter-period phase difference between successive legs while in a trot, pairs of diagonal legs strike the ground simultaneously with a half-period phase difference with the other diagonal pair of legs. The phase shifts for the primary gaits of walk, trot, and pace are listed in Table 1 in terms of the output $u_1(t)$ from cell 1.

Table 1. Phase shifts of primary gaits.

Legs		Walk		Rrot		Pace	
3	4	$u_1(t+\frac{1}{4})$	$u_1(t+\frac{3}{4})$	$u_1(t+\frac{1}{2})$	$u_1(t)$	$u_1(t)$	$u_1(t+\frac{1}{2})$
1	2	$u_1(t)$	$u_1(t+\frac{1}{2})$	$u_1(t)$	$u_1(t+\frac{1}{2})$	$u_1(t)$	$u_1(t+\frac{1}{2})$
Legs		Jump		Bound		Pronk	
3	4	$u_1(t)$	$u_1(t)$	$u_1(t+\frac{1}{2})$	$u_1(t+\frac{1}{2})$	$u_1(t)$	$u_1(t)$
1	2	$u_1(t+\frac{1}{4})$	$u_1(t+\frac{1}{4})$	$u_1(t)$	$u_1(t)$	$u_1(t)$	$u_1(t)$

Figure 2 shows numerical simulations from the model CPG of [15] that illustrate a walk and a trot. Note the quarter-period phase shift from u_1 to u_3 to u_2 to u_4 in the walk. Additional discussion of numerical simulations is given in Section 6.

1.4. Why four cells do not suffice

Networks of four symmetrically coupled cells are used in [9] to model the CPGs of quadrupeds, each cell sending an output signal to a corresponding limb. Periodic solutions in the four-cell networks correspond to different gait patterns of quadrupeds. The networks studied in [9] have the following property: if walk, trot, and pace periodic solutions are present in the network, then trot and pace are symmetrically related periodic solutions.

Suppose that two different gait patterns are modeled by symmetrically related periodic solutions, also called conjugate periodic solutions. Then the periodic solutions exist simultaneously and have the same stability properties. However, there is evidence indicating that trot and pace do not exist simultaneously and evidence indicating that they do not have the same stability properties. First, camels and giraffes use the pace for locomotion at slow and intermediate speeds, but do not trot; while horses are known to trot, but unless taught, do not use the pace. See [22] p. 705 or [18] p. 274. Therefore, the CPG of the camel selects pace but suppresses trot, and the horse CPG selects trot but unless taught suppresses pace. Second, results from Blaszczyk and Dobrzecka [2] indicate that the stability of pace and trot are not the same. In [2], it is reported that puppies use a trot gait at intermediate speed. In their experiment, the puppies' legs are restrained as they make their first steps, so that they can only use a pace at intermediate speeds — not a trot. Different dogs retain this device for amounts of time ranging from 2 to 6 months. In post-restraint trials it is reported that dogs that were in the shorter restraint period switched back to a trot quickly with only occasional use of a pace. In the longer restrained animals, occurrence of pace was more frequent but the use of pace decreased with every post-restraint experimental trial. Therefore, as in [15], we make the assumption that different gait patterns are modeled by periodic solutions that are nonconjugate.

1.5. Symmetry in the eight-cell network

The symmetry group of the network in Figure 1 is the abelian group $\mathbf{Z}_4 \times \mathbf{Z}_2$. We make the modeling assumption that a cell in the network sends its signal to only one leg. In order for this network to model observed quadrupedal gaits it is necessary that the output signals to the four legs are sent by the top four cells in Figure 1. Assuming that cell 1 sends its signal to the left hind leg, it follows that cell 2 sends its signal to the right hind leg, cell 3 to the left fore leg, and cell 4 to the right fore leg. A possible explanation for the role of the bottom part of the network is discussed in [16] where it is argued, based on observations of the human gaits walk and run, that the signals are sent to muscle groups rather than to legs. See also the explanation before Theorem 3.3.

In [15], it is shown that this quadruped network can model trot, pace, and walk, without introducing unwanted conjugacies between the periodic solutions.

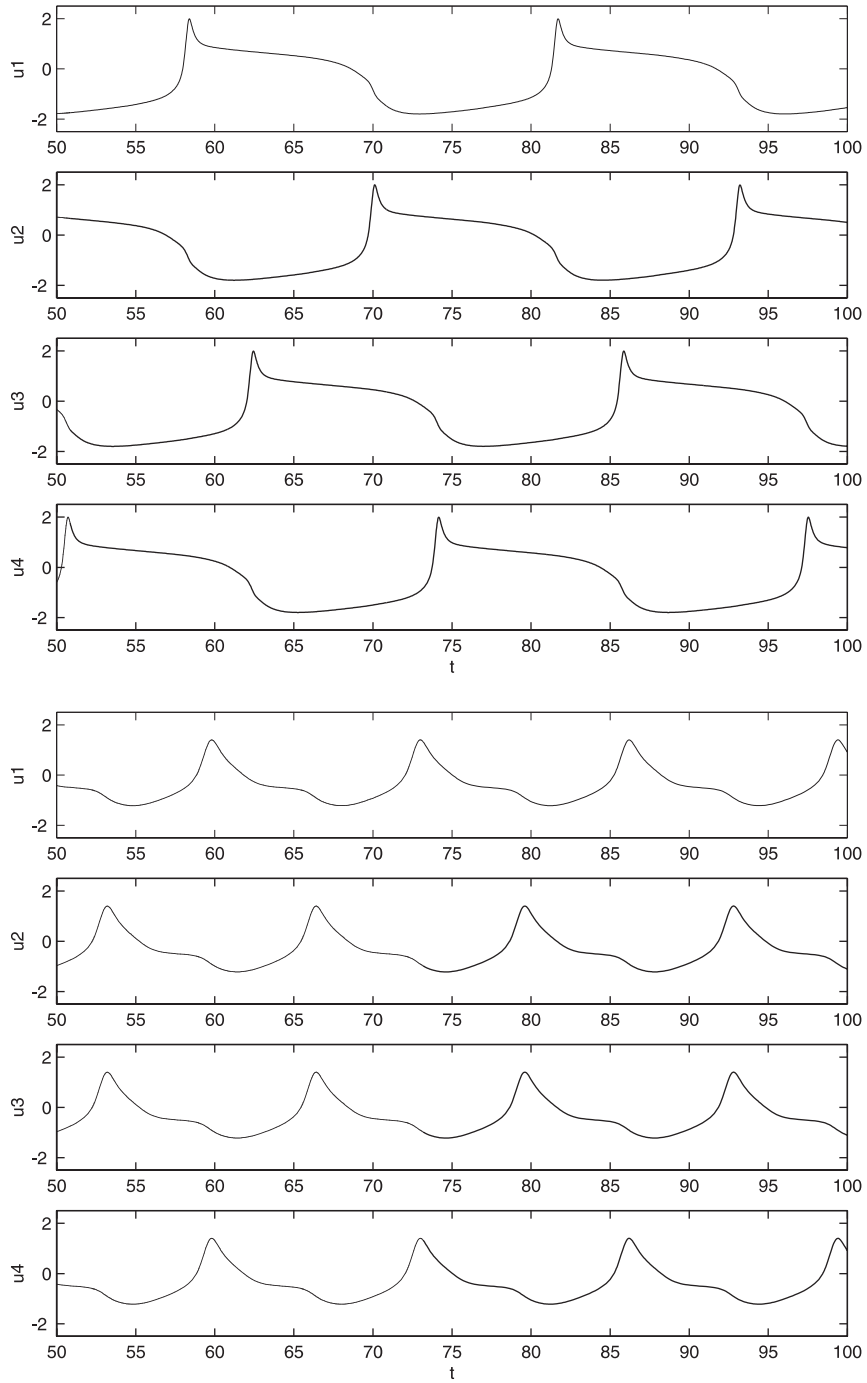

Fig. 2. Signal u_1 goes to the left hind leg; u_2 goes to the right hind leg; u_3 goes to the left fore leg; and u_4 goes to the right fore leg. Top: walk. Bottom: trot.

The absence of conjugacy follows from the fact that $\mathbf{Z}_4 \times \mathbf{Z}_2$ is abelian. A *stand* equilibrium of the network is an equilibrium that is fixed by all symmetries of the network. Since $\mathbf{Z}_4 \times \mathbf{Z}_2$ is abelian, generically the nonreal eigenvalues of the linearization of the system of ordinary differential equations of the network are simple. Then, periodic solutions modeling the quadruped gaits can be produced by simple Hopf bifurcation from equilibria. All periodic solutions that bifurcate from stand by simple Hopf bifurcation are primary gaits.

1.6. New results concerning the eight-cell network

We continue the study of the quadruped network in two directions. First, we show that the quadruped network with $\mathbf{Z}_4 \times \mathbf{Z}_2$ symmetry is the smallest one that produces walk, trot, and pace as nonconjugate periodic solutions. To prove this result, we classify the possible spatio-temporal symmetry groups of a Γ-equivariant vector field when Γ is finite. Based on the idea that signals go from cells to muscle groups (as discussed in [16]), we also show how to make a natural assignment of cells to legs for all eight cells in our network. See Theorem 3.3. This theorem leads to the two networks shown in Figure 6. These networks have the same symmetries and are dynamically equivalent to the one in Figure 1.

Second, suppose that the cells are two-dimensional and the coupling of the network is *linear synaptic*. Suppose also that the cell dynamics has an equilibrium and the linearization at the equilibrium has nonreal eigenvalues. Then, we show that all primary gaits (except pronk) can be made to bifurcate from a stand equilibrium by varying only coupling parameters. For certain gaits (trot, pace, and bound) we show that these bifurcations can lead to stable periodic solutions. Moreover, by numerical exploration all primary gaits can be found to occur as stable periodic solutions.

The complexity of the central nervous system of mammals has prevented a detailed description of the CPG for locomotion. Since our proof of existence of primary gaits depends only on the existence of an equilibrium for the cell dynamics with linearization having nonreal eigenvalues, our result is robust; it does not depend explicitly on biological details of the animal's central nervous system.

1.7. Structure of the paper

In Section 2 and Appendix A, we determine the possible spatio-temporal symmetry groups of time periodic solutions when Γ is finite. In Section 3, we use the results of Section 2 to prove Theorem 3.2, from which it follows that the quadruped network with $\mathbf{Z}_4 \times \mathbf{Z}_2$ symmetry is the smallest network modeling walk, trot, and pace without conjugacies. In Section 4, we state the theorems of existence and stability of periodic solutions from Hopf bifurcation. In Section 5, we prove the existence and stability results stated in Section 4. Numerical simulations using the dimensionless Morris-Lecar equations [30, 34] as cell dynamics are presented in Section 6 and a summary is given in Section 7.

2. Robust periodic solutions

In this section and in Appendix A we discuss the spatio-temporal symmetries of periodic solutions in symmetric systems of differential equations. Additional background may be found in [17]. We also discuss the conditions under which the periodic solution and its symmetries are robust to small parameter changes, which, as is discussed below, is an important consideration in gait CPG modeling.

We begin by defining the symmetries of a differential equation and the spatio-temporal symmetries of periodic solutions, and then, as in [15], relate these symmetries to gaits.

Let $\Gamma \subset \mathbf{O}(n)$ be a finite group acting on $\mathbf{R}^n$ and let $f : \mathbf{R}^n \to \mathbf{R}^n$ be a smooth Γ-equivariant vector field, that is,

$$f(\gamma x) = \gamma f(x) \quad \forall \gamma \in \Gamma.$$

2.1. Spatio-temporal symmetries

Each symmetry of a periodic solution $U(t)$ to the system of differential equations

$$\frac{dU}{dt} = f(U) \tag{2.1}$$

is a combination of spatial and temporal. For simplicity in exposition we assume that our periodic solutions are 1-periodic. Let $\gamma \in \Gamma$; by equivariance $\gamma U(t)$ is also a solution to (2.1). Uniqueness of solutions to initial conditions in (2.1) implies that there are two possibilities: either the trajectories $\{\gamma U(t)\}$ and $\{U(t)\}$ are identical or they are disjoint. In the former case, uniqueness of solutions also implies that there is a phase shift θ such that

$$\gamma U(t) = U(t - \theta).$$

See [17] for details. Then the phase shift θ can be thought of as an element of the circle group $\mathbf{S}^1$ by identifying $\mathbf{S}^1 = [0, 1)$. The pair

$$(\gamma, \theta) \in \Gamma \times \mathbf{S}^1$$

is a *spatio-temporal* symmetry of $U(t)$; and the collection of all spatio-temporal symmetries of $U(t)$ forms a subgroup $\Delta \subset \Gamma \times \mathbf{S}^1$.

As illustrated in Table 1, standard quadruped gaits are time periodic states with certain well-defined phase shifts. Following [15] we show how these phase shifts can be derived from the symmetries of associated periodic solutions in our CPG model (Figure 1). The symmetry group of the network shown in Figure 1 is $\mathbf{Z}_4(\omega) \times \mathbf{Z}_2(\kappa)$ generated by the four-cycle ω that permutes cells around the ring and the two-cycle κ that interchanges left cells with right cells. We can define each primary gait by associating phase shifts to ω and κ, as in Table 2. For example, suppose $U(t) = (u_1(t), \ldots, u_8(t))$ is a periodic solution with the spatio-temporal symmetries of a trot. Then $(\kappa, \frac{1}{2})$ symmetry implies that $u_2(t) = u_1(t + \frac{1}{2})$ and $u_4(t) = u_3(t + \frac{1}{2})$. Similarly, $(\omega, \frac{1}{2})$ implies $u_3(t) = u_1(t + \frac{1}{2})$ and $u_4(t) = u_2(t + \frac{1}{2})$. In this way a trot solution has the form indicated in Table 1.

Table 2. Symmetries of primary gaits.

Gait	Pronk	Pace	Bound	Trot	Jump	Walk
ω phase shift	0	0	$\frac{1}{2}$	$\frac{1}{2}$	$\frac{1}{4}$	$\frac{1}{4}$
κ phase shift	0	$\frac{1}{2}$	0	$\frac{1}{2}$	0	$\frac{1}{2}$

There is a second and equivalent way to view spatio-temporal symmetries. Let $H \subset \Gamma$ consist of symmetries that preserve the trajectory of U; that is, $\gamma \in H$ if

$$\gamma\{U(t)\} = \{U(t)\}.$$

As noted previously, if $\gamma \in H$, then there exists $\theta \in \mathbf{S}^1$ such that (γ, θ) is a spatio-temporal symmetry of $U(t)$. Moreover, the map $\varphi : H \to \Gamma \times \mathbf{S}^1$ defined by $h \to (h, \theta)$ is an isomorphism of H onto Δ.

Thus, spatio-temporal subgroups $\Delta \subset \Gamma \times \mathbf{S}^1$ are isomorphic to subgroups of Γ. Next we show that these subgroups have additional algebraic structure. Let $K \subset \Gamma$ be the group of purely *spatial symmetries* of $U(t)$; that is, $\gamma \in K$ if

$$\gamma U(t) = U(t)$$

for all t. It is clear that $K \subset H$. Moreover, the map $\Theta : H \to \mathbf{S}^1$ defined by $\Theta(h) = \theta$ where (h, θ) is a spatio-temporal symmetry of $U(t)$ is a group homomorphism with kernel K. It follows that the quotient group H/K is isomorphic to a finite subgroup of $\mathbf{S}^1$. Therefore,

$$H/K \cong \mathbf{Z}_m \tag{2.2}$$

for some integer $m \geq 0$. Thus, spatio-temporal subgroups of $\Gamma \times \mathbf{S}^1$ can be identified with pairs of subgroups $K \subset H$ of Γ satisfying (2.2). For example, for a periodic solution corresponding to a trot, $K = \mathbf{Z}_2(\omega\kappa)$ and $H = \mathbf{Z}_4 \times \mathbf{Z}_2$.

2.2. Symmetry - generated subgroups

Definition 2.1. *A hyperbolic periodic solution $U(t) \in \mathbf{R}^n$ of (2.1) with spatio-temporal symmetry subgroup Δ is* robust *if periodic solutions obtained from $U(t)$ by small Γ-equivariant perturbations of (2.1) also have spatio-temporal symmetry subgroup Δ.*

The subgroup $\Delta \subset \Gamma \times \mathbf{S}^1$ is symmetry generated *(for the action of Γ on $\mathbf{R}^n$) if there is a robust periodic solution for some Γ-equivariant system of differential equations on $\mathbf{R}^n$ whose spatio-temporal symmetry subgroup is Δ.*

The following theorem, which is proved in Appendix A, classifies symmetry generated subgroups (and hence the types of spatio-temporal symmetry of robust periodic solutions) for coupled cell systems of the kind we consider.

Theorem 2.2. *Let $K \subset H \subset \Gamma$ be subgroups where Γ is the symmetry group of a coupled cell system. Assume that*

(a) the order of Γ *equals the number of cells and every cell is mapped to any other cell by a symmetry, and*
(b) the dynamics of each cell is at least two-dimensional.

Then robust periodic solutions whose spatial symmetries are K *and whose spatio-temporal symmetries are* H *exist only if (2.2) is valid.*

Note that the eight-cell network pictured in Figure 1 with symmetry group $\mathbf{Z}_4 \times \mathbf{Z}_2$ satisfies the hypotheses of Theorem 2.2. Therefore, we can enumerate all the types of spatio-temporal symmetry that any periodic solution to any system of differential equations based on this network can have, as was done in [15], Table 4. In Section 4 we use Hopf bifurcation to produce robust periodic solutions for this eight-cell model.

2.3. An example with $\mathbf{D}_4$ *symmetry*

We need the following example when discussing the uniqueness of the eight-cell gait model in Section 3. Consider the eight-cell system shown in Figure 3 having permutation group $\mathbf{D}_4$. (Note the arrows go in opposite directions around the two rings in this network.)

Geometrically $\mathbf{D}_4$ is the symmetry group of a square and is generated by a four-cycle ω corresponding to rotation counterclockwise by 90° and a reflection κ whose line of reflection connects midpoints of opposite sides of the square. Note that $\kappa\omega$ is a reflection whose line of symmetry connects opposite vertices of the square. There are eight conjugacy classes of subgroups of $\mathbf{D}_4$:

$$\begin{array}{cccc} \mathbf{D}_4 & \mathbf{D}_2^s = \langle \kappa, \omega^2, \kappa\omega^2 \rangle & \mathbf{D}_2^p = \langle \kappa\omega, \omega^2, \kappa\omega^3 \rangle & \mathbf{Z}_4 = \langle \omega \rangle \\ \mathbf{1} & \mathbf{Z}_2^s = \langle \kappa \rangle & \mathbf{Z}_2^p = \langle \kappa\omega \rangle & \mathbf{Z}_2 = \langle \omega^2 \rangle \end{array}$$

Figure 4 illustrates the containment relations between these subgroups.

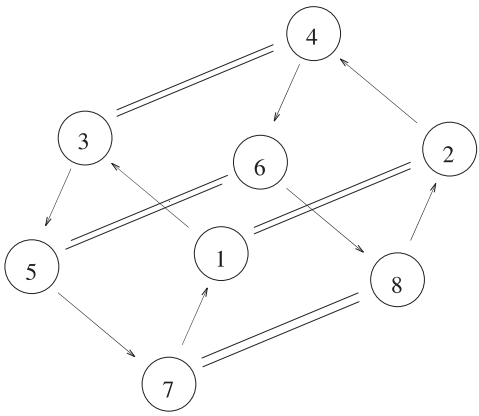

Fig. 3. Eight-cell network with $\mathbf{D}_4$ symmetry.

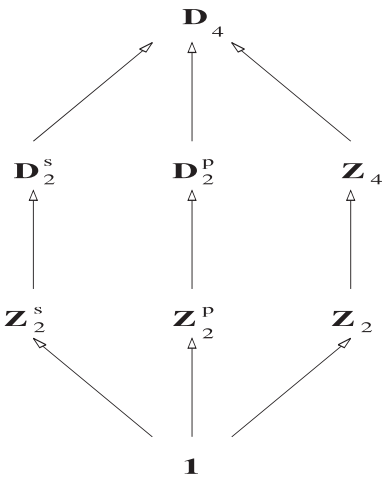

Fig. 4. Lattice of subgroups of $\mathbf{D}_4$.

When the internal dynamics is at least two-dimensional, Theorem 2.2 there are 12 types of robust periodic solutions with nontrivial temporal symmetries ($H \supsetneq K$) in this coupled cell system, and they are:

$$\begin{array}{cccc}
\mathbf{Z}_4 \subset \mathbf{D}_4 & \mathbf{D}_2^p \subset \mathbf{D}_4 & \mathbf{D}_2^s \subset \mathbf{D}_4 & \mathbf{Z}_2 \subset \mathbf{Z}_4 \\
\mathbf{Z}_2 \subset \mathbf{D}_2^p & \mathbf{Z}_2^p \subset \mathbf{D}_2^p & \mathbf{Z}_2 \subset \mathbf{D}_2^s & \mathbf{Z}_2^s \subset \mathbf{D}_2^s \\
\mathbf{1} \subset \mathbf{Z}_4 & \mathbf{1} \subset \mathbf{Z}_2 & \mathbf{1} \subset \mathbf{Z}_2^p & \mathbf{1} \subset \mathbf{Z}_2^s
\end{array}$$

Note that there is only one symmetry generated subgroup that can correspond to a robust periodic solution with a quarter-period phase shift and that subgroup is given by the pair $\mathbf{1} \subset \mathbf{Z}_4$.

3. CPG network for quadruped locomotion

The CPG network for quadruped locomotion is shown in Figure 1. The arrows in Figure 1 determine the nearest neighbor coupling between the cells as well as the symmetry of the network. In principle, there can be as many couplings in this network as desired, as long as the couplings respect the symmetry group of the network. That is, each coupling generates a group orbit of couplings, and the couplings must not change the symmetry group of the network. For instance, it is possible to have bidirectional coupling between neighboring cells in the rings, as long as the coupling in one direction is different from the coupling in the opposite direction.

In order to understand why an eight-cell network is the simplest network that can describe quadruped locomotion, we make explicit the modeling assumptions that preclude four-cell networks. Two of our modeling assumptions are:

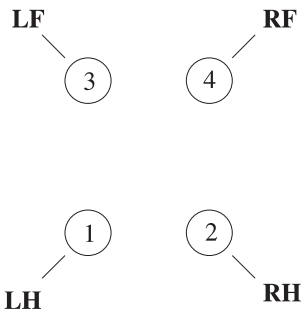

Fig. 5. Schematic four-cell network for gaits in four-legged animals.

(A1) Each cell in the CPG network sends its signal to only one leg.
(A2) Different gaits are modeled by nonconjugate periodic solutions.

Consider the four-cell network of Figure 5. By (A1) we can identify each cell with a leg and without loss of generality we can assume that the signal from cell 1 goes to the left hind leg. Suppose that the four-cell network produces a walk. In a quadruped walk the animal moves its left hind leg, then its left fore leg, then its right hind leg, and then its right fore leg — each with a quarter-period phase shift. Since symmetries of this network are permutations of the four cells followed by a phase shift, it follows that there must be a four-cycle that is associated with the walk. By renumbering the cells, if necessary, we can assume that that four-cycle is (1 3 2 4). It then follows that cell 3 must send its signal to the left fore leg, cell 2 to the right hind leg, and cell 4 to the right fore leg, as shown in Figure 5.

A trot is a gait in which the diagonal legs move synchronously; that is, the permutation (14)(23) is a symmetry of a trot. Both a trot and a pace are gaits where interchanging left and right legs is associated with a half-period phase shift; that is, a symmetry of these gaits is the permutation (12)(34) followed by a half-period phase shift. Finally, in the pace gait the animal moves its left legs and its right legs synchronously. Therefore, the permutation (13)(24) is a symmetry of a pace. We emphasize that the quarter-period phase shift of the walk, and the half-period phase shift of trot and pace is exact even under parameter perturbations. We make this additional assumption.

(A3) The network has robust periodic solutions that model walk, trot, and pace.

Theorem 3.1 ([15]). *Suppose that the four-cell network satisfies (A1), (A2), and (A3). Then trot and pace are conjugate solutions.*

Proof. Let $\Gamma \subset \mathbf{S}_4$ be the symmetry group of the network. Since the walk is robust, the four-cycle $(1324) \in \Gamma$. Suppose that the subgroups corresponding to trot and pace are symmetry generated, then $(12)(34) \in \Gamma$. Moreover, trot implies $(14)(23) \in \Gamma$ and pace implies $(13)(24) \in \Gamma$. Note that

$$(1324) \cdot (14)(23) \cdot (1324)^{-1} = (13)(24)$$

$$(1324)\cdot(13)(24)\cdot(1324)^{-1} = (14)(23)$$
$$(1324)\cdot(12)(34)\cdot(1324)^{-1} = (12)(34).$$

Thus, (1324) conjugates the generators of the symmetry groups of trot and pace and these subgroups are conjugate. □

The consequence of Theorem 3.1 is that four-cell networks cannot model walk, trot, and pace unless trot and pace are conjugate periodic solutions. Therefore, we must consider symmetric cell systems with more than four cells.

From [15], we know that there exists a cell to leg assignment for an eight-cell network with $\mathbf{Z}_4 \times \mathbf{Z}_2$ symmetry of Figure 1 that can produce nonconjugate walk, trot, and pace robust periodic solutions. Theorem 3.2 shows that the eight-cell quadruped network with $\mathbf{Z}_4 \times \mathbf{Z}_2$ symmetry is the smallest network that can model walk, trot, and pace without unwanted conjugacies. To prove this result we make an additional assumption.

(A4) The symmetry group of the coupled cell network acts *transitively* on the cells; that is, every cell can be mapped to any other cell by a symmetry.

Theorem 3.2. *Let $\mathcal{N}$ be a Γ-symmetric cell network. Assume that $\mathcal{N}$ is a network satisfying (A1), (A2), (A3), and (A4) with minimum $|\Gamma|$. Then $\mathcal{N}$ is the quadruped eight-cell network with $\Gamma = \mathbf{Z}_4 \times \mathbf{Z}_2$.*

Proof. The group Γ must contain at least a four-cycle permutation ω to account for the quarter-period phase shift of the walk and ω must permute the signals sent to the four legs. Thus the network contains at least four cells, say cells 1,3,5,7 which ω permutes cyclically. Pace and trot have a half-period phase shift between left and right; so Γ must contain a transposition, say κ. There are three possible cases: either $\kappa = \omega^2$, κ and ω commute, or κ and ω do not commute. We consider the three possibilities in turn.

Suppose that $\kappa = \omega^2$, then $\Gamma = \mathbf{Z}_4$. Transitivity then implies that the network has four cells which is ruled out by Theorem 3.1.

Next, suppose that κ and ω commute. Since $\kappa \neq \omega^2$, there exists a fifth cell, labeled 2, such that κ interchanges cell 1 with cell 2. Since $\kappa\omega = \omega\kappa$, then κ must send cell 3 where ω sends cell 2; label this sixth cell 4. Repeating the above argument with $\kappa\omega = \omega\kappa$ shows that there is a second ring of four cells. Thus, we obtain the quadruped network with $\mathbf{Z}_4 \times \mathbf{Z}_2$ symmetry.

Finally, suppose that κ and ω are noncommuting permutations: they generate the group $\mathbf{D}_4$. Since $|\Gamma|$ is minimal, $\Gamma = \mathbf{D}_4$. Transitivity implies that the network has four or eight cells, and the case of four cells is ruled out by Theorem 3.1.

Suppose that $U(t)$ is a 1-periodic solution to the differential equations in the eight-cell system that models a walk. A walk is characterized by permuting the legs from left rear to left front to right rear to right front coupled with a quarter-period phase shift. For walk to be modelled by a robust periodic solution, there must be a four-cycle in the group that induces the quarter-period phase shift on $U(t)$. There are two possible four-cycles in $\mathbf{D}_4$ — ω and ω^3. Since these four-cycles are conjugate, we may choose either one to induce the quarter-period phase shift in the walk

— and we choose ω. So

$$\omega U(t) = U\left(t - \frac{1}{4}\right). \tag{3.1}$$

Transitivity of $\mathbf{D}_4$ implies that the eight cells divide into two rings of four cells that are cyclicly permuted by ω. See Figure 3. We can number these cells so that

$$\omega = (1\ 3\ 5\ 7)(2\ 4\ 6\ 8).$$

Transitivity of $\mathbf{D}_4$ implies that κ must permute the two rings of four cells that are permuted by ω. We can choose cell 2 so that κ permutes cells 1 and 2. It follows from the identity $\kappa\omega = \omega^3\kappa$ that

$$\kappa = (1\ 2)(3\ 8)(5\ 6)(7\ 4).$$

Suppose that we write the walk solution

$$U(t) = (u_1(t), \ldots, u_8(t))$$

where $u_j(t)$ denotes the output from cell j. It follows from (3.1) that

$$u_3(t) = u_1\left(t - \frac{1}{4}\right), \qquad u_5(t) = u_1\left(t - \frac{1}{2}\right), \qquad u_7(t) = u_1\left(t - \frac{3}{4}\right)$$

and

$$u_4(t) = u_2\left(t - \frac{1}{4}\right), \qquad u_6(t) = u_2\left(t - \frac{1}{2}\right), \qquad u_8(t) = u_2\left(t - \frac{3}{4}\right).$$

We can number the cells so that cell 1 sends its signal to the left hind leg. It follows that the signal from cell 3 is sent to the left fore leg, the signal from cell 5 is sent to the right hind leg, and the signal from cell 7 is sent to the right fore leg.

Next we explore the implications of existence of a symmetry generated 1-periodic solution $V(t) = (v_1(t), \ldots, v_8(t))$ that represents either a trot or a pace. The trot and pace solutions have the half-period phase shift between signals to the left and right legs. Pace has the same signal going to front legs and hind legs, and trot has the same signal going to pairs of diagonal legs.

It follows from κ symmetry that

$$\begin{aligned} v_2(t) &= v_1\left(t + \tfrac{1}{2}\right) \\ v_4(t) &= v_7\left(t + \tfrac{1}{2}\right) \\ v_6(t) &= v_5\left(t + \tfrac{1}{2}\right) \\ v_8(t) &= v_3\left(t + \tfrac{1}{2}\right). \end{aligned}$$

Note that κ is contained in a unique subgroup of $\mathbf{D}_4$ that is isomorphic to $\mathbf{D}_2$, namely $\mathbf{D}_2(\kappa, \omega^2, \kappa\omega^2)$. There is also a unique subgroup of $\mathbf{D}_4$ that is isomorphic to $\mathbf{D}_2$ and which does not contain κ, namely, $\mathbf{D}_2(\kappa\omega, \omega^2, \kappa\omega^3)$. Therefore, the classification of robust periodic solutions in Section 2 shows that there are three possible types

of periodic solutions having κ as a spatio-temporal symmetry with a half-period phase shift and also having a nontrivial spatial symmetry. They are:

$$\begin{aligned}\mathbf{D}_2(\kappa\omega, \omega^2, \kappa\omega^3) &\subset \mathbf{D}_4\\ \mathbf{Z}_2(\omega^2) &\subset \mathbf{D}_2(\kappa, \omega^2, \kappa\omega^2)\\ \mathbf{Z}_2(\kappa\omega^2) &\subset \mathbf{D}_2(\kappa, \omega^2, \kappa\omega^2)\end{aligned}$$

The restrictions on the signals going to each cell in each of these symmetry types of solutions are:

RF	$v_1\left(t+\frac{1}{2}\right)$	7 8	$v_1(t)$
RH	$v_1(t)$	5 6	$v_1\left(t+\frac{1}{2}\right)$
LF	$v_1\left(t+\frac{1}{2}\right)$	3 4	$v_1(t)$
LH	$v_1(t)$	1 2	$v_1\left(t+\frac{1}{2}\right)$
RF	$v_3(t)$	7 8	$v_3\left(t+\frac{1}{2}\right)$
RH	$v_1(t)$	5 6	$v_1\left(t+\frac{1}{2}\right)$
LF	$v_3(t)$	3 4	$v_3\left(t+\frac{1}{2}\right)$
LH	$v_1(t)$	1 2	$v_1\left(t+\frac{1}{2}\right)$
RF	$v_3\left(t+\frac{1}{2}\right)$	7 8	$v_3\left(t+\frac{1}{2}\right)$
RH	$v_1\left(t+\frac{1}{2}\right)$	5 6	$v_1(t)$
LF	$v_3(t)$	3 4	$v_3(t)$
LH	$v_1(t)$	1 2	$v_1\left(t+\frac{1}{2}\right)$

The cells to legs assignment for the right cells is also restricted by the walk. Hence suppose that cell 4 sends its output signal to the left hind leg, then we have two possible assignments: 4-LH, 6-LF, 8-RH, 2-RF or 4-LH, 2-LF, 8-RH, 6-RF. We can choose either one of the above assignments to illustrate the remainder of the proof. Note, however, that regardless of the assignment of cells to legs on the right hand side, we can rule out the three periodic solutions shown above. In the first and second periodic solutions, the signals sent to the left hind leg and the right hind leg are in-phase. Therefore they cannot be either a pace or a trot. The third periodic solution is a candidate for either a pace or a trot because of the half-period phase shift between left hind and right hind. Since pace and trot are nonconjugate, this symmetry type cannot model both trot and pace. Hence, robust periodic solutions modelling walk, trot, and pace do not coexist in this network. □

Note that there exists an eight-cell network that consists of two disjoint four-cell networks which produces nonconjugate symmetry generated walk, trot, and pace periodic solutions. One subnetwork is a four-cell network with $\mathbf{Z}_4$ symmetry that models walk, and the other is a four-cell network with $\mathbf{D}_2$ symmetry that models pace and trot, see [9]. Periodic solutions of this network have symmetry groups

Table 3. Cell to leg assignment in Figure 1.

7	8		LH	RH
5	6		LF	RF
		→		
3	4		LF	RF
1	2		LH	RH

based on $\mathbf{Z}_4 \times \mathbf{D}_2$. In this eight-cell network, signals can be sent to the legs simultaneously from each subnetwork. So, modeling of quadruped CPG with two four-cell models requires the existence of an external control that determine which gait is sent to the legs.

The existence of an external control for the CPG does not seem to be justified by the physiological data. It is known that external controls from the cerebellum to the CPG contribute to the coordination of gaits. It seems that these signals are not necessary, since less coordinated locomotion can be carried out even after cerebelloctomy, see Grillner [19] p. 1207-1208. Note that there is evidence that the initiation and control of the CPG for locomotion depends on a variety of signals coming from the brain stem, see [19] p. 1209-1213. However, much evidence shows that the CPG has enough flexibility to produce different locomotor behavior even in the absence of inputs from the brain or peripheral feedback, Grillner [19] p. 1213 and Pearson [31] p. 270. Hence, the two independent network CPG model is too restrictive.

Theorem 3.2 shows that there is only one possible eight-cell network that can produce the nonconjugate gaits walk, trot, and pace, and that this network has $\mathbf{Z}_4 \times \mathbf{Z}_2$ symmetry. We proved this theorem assuming that the signal from each cell is transmitted to precisely one leg. So far, however, we have not discussed how the assignment of cells to legs is made in this abelian network. There are a number of different and consistent ways in which the cell to leg assignment can be made of which the assignment implicit in Figure 1 is only one. In [15] we assumed that the signals from cells to legs is the one given in Table 3.

In our discussions in [15] we assumed that the top four cells $(1, \ldots, 4)$ controlled the gait rhythms and that, in effect, the bottom four cells $(5, \ldots, 8)$ served only the role of correctly propagating the signals. Under this assumption there are many different ways to make the leg assignment of cells $5, \ldots, 8$ that are consistent with the network symmetry. In [16], however, we discussed evidence suggesting that each cell signals a particular muscle group in a particular leg. Since each joint is controlled by two primary muscle groups (flexors and extensors), this may explain physiologically why the doubled-up eight-cell network, as opposed to a four-cell network, is needed to produce walk, trot, and pace. If this supposition is correct, then there is a natural restriction to put on the cell to leg assignments, as we now explain. Moreover, with this restriction, there exist only two possible cell to leg assignments.

Suppose that $F : cells \to legs$ is a possible assignment. We assume that each leg is assigned two cells and, without loss of generality, we can assume that

$F(1) = LH$, that is, one of the two cells that is assigned to the left hind leg is cell 1. Based on the cell to muscle group interpretation of a CPG a reasonable assumption about F states that if the signals from cells i and j are sent to the same leg, then for any network symmetry γ the signals from cells γi and γj are also sent to the same leg. In symbols:

$$\text{If } F(i) = F(j), \text{ then } F(\gamma i) = F(\gamma j). \tag{3.2}$$

With this assumption we prove that there are precisely two different assignments of cells to legs.

Theorem 3.3. *Assume that the cell to leg assignment F satisfies $F(1) = LH$ and (3.2). Then F is one of the two cell to leg assignments given in Table 4.*

Proof. As in the proof of Theorem 3.2 the four-cycle permutation ω accounts for the quarter-period phase shift of the walk and the transposition κ accounts for the half-period phase shift between left and right in the trot and pace. Transitivity of the group $\mathbf{Z}_4 \times \mathbf{Z}_2$ implies that ω permutes cyclically four cells that we can number 1,3,5,7.

Since κ and ω commute and $\kappa \neq \omega^2$, there exists a fifth cell, labeled 2, such that κ interchanges cell 1 with cell 2. It follows that

$$\omega = (1\ 3\ 5\ 7)(2\ 4\ 6\ 8) \quad \text{and} \quad \kappa = (1\ 2)(3\ 4)(5\ 6)(7\ 8).$$

We assume for definiteness that the signal from cell 1 goes to the left hind leg. Since κ reflects the interchange of left with right in the trot, the signal from cell 2 must be sent to the right hind leg. Similarly, since ω is responsible for the quarter-period phase shift in the walk, the signal from cell 3 must be sent to the left fore leg and then κ implies that the signal from cell 4 is sent to the right fore leg.

In principle, the signal from cell 5 can be sent to any of the four legs. It is straightforward to check that if the signal from cell 5 is sent to either the left hind or the right hind leg, then (3.2) forces the leg assignments given in Table 4.

If the signal from cell 5 is sent to either the left fore or the right fore leg, then (3.2) forces a contradiction. First, if that signal is sent to the left fore leg, then since ω maps cell 3 to cell 5 it must map left fore leg cells to left fore leg cells by (3.2). Therefore, the signal from cell 7 (which is mapped by ω from cell 5) must also be sent to the left fore leg. Moreover, applying ω once again shows that the signal from cell 1 must also be sent to the left fore leg, contradicting the assumption that

Table 4. Cell to leg assignments in Theorem 3.3.

7	8		LF	RF			7	8		RF	LF
5	6		LH	RH			5	6		RH	LH
		→			and			→			
3	4		LF	RF			3	4		LF	RF
1	2		LH	RH			1	2		LH	RH

the signal from cell 1 is sent to the left hind leg. Second, suppose that signal is sent to the right fore leg. Since ω maps cells 3 to 5 and 2 to 4, it follows that ω maps cells assigned to the left fore leg (3) and the right hind leg (2) to cells assigned to the right fore leg (5 and 4), which contradicts assumption (3.2). □

We call the first network listed in Table 4 the *zig-zag network* and the second the *criss-cross network*. These networks are illustrated in Figure 6. See Section 7 for additional discussion of the differences between the zig-zag and criss-cross networks.

4. Existence and stability of primary gaits

The general form of the coupled cell system that we analyze is:

$$\dot{u}_j = F(u_j) + \sum_{i \to j} A_{ij} H(u_i, u_j) \tag{4.1}$$

where u_j denotes the state variables in cell j, F denotes the internal dynamics of the cell, H denotes the coupling from cell i to cell j, A_{ij} denotes coupling strengths, and the sum is taken over those cells i that are coupled to cell j.

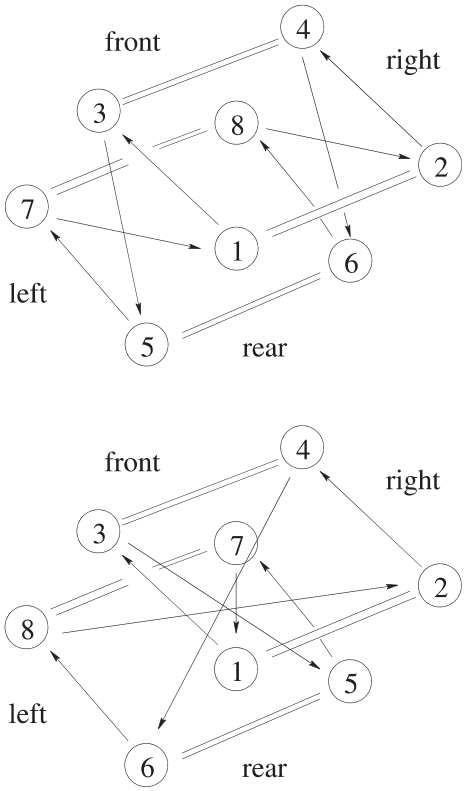

Fig. 6. Schematic eight-cell networks for gaits in four-legged animals consistent with (3.2). Top: The zig-zag network. Bottom: The criss-cross network.

We now discuss how to find robust periodic solutions in the eight-cell CPG model by utilizing Hopf bifurcations from a stand equilibrium. As was shown in [15], the cell dynamics must be at least two-dimensional in order to have Hopf bifurcation to a trot. Indeed, it can be proved using Theorem A.1 that robust trots cannot occur in any eight-cell system having one-dimensional cell dynamics. We assume that the cells have two-dimensional internal dynamics. We denote $F = (f, g)$ in coordinates where $f, g : \mathbf{R}^2 \to \mathbf{R}$ are smooth nonlinear functions. Then the internal cell dynamics is given by

$$\begin{aligned} \dot{x} &= f(x, y) \\ \dot{y} &= g(x, y). \end{aligned} \tag{4.2}$$

In this notation, we suppress the explicit dependence of f and g on parameters.

Following Kopell and Ermentrout [25] we say that the coupling function in (4.1) is *diffusive* if $H(u, u) = 0$ for all $u \in \mathbf{R}^2$. Otherwise, H is called *synaptic*. In this paper we discuss only synaptic coupling; similar results are valid for diffusive coupling and may be found in [4]. In our analyses we assume that the coupling function has the form $H(u_i, u_j) = (h(x_i, x_j), h(y_i, y_j))$ where in the case of *linear* synaptic coupling $h(x_i, x_j) = x_i$.

The system of equations from the quadruped network is constructed as follows. Suppose that the coupling of the quadruped network is given by nearest neighbor coupling only; that is, the coupling shown in Figure 1. Let α, β be the parameters controlling the ipsilateral coupling strength and γ, δ be the parameters that control the contralateral coupling strength. From Figure 1, we see that the dynamical activity of cell 7 and cell 2 contribute to the dynamics of cell 1 through ipsilateral and contralateral coupling, respectively. Similarly, cell 8 and cell 1 contribute to the dynamics of cell 2. The equations for the dynamics of cell 1 and 2 are therefore given by

$$\begin{aligned} \dot{x}_1 &= f(x_1, y_1) + \alpha h(x_7, x_1) + \gamma h(x_2, x_1) \\ \dot{y}_1 &= g(x_1, y_1) + \beta h(y_7, y_1) + \delta h(y_2, y_1) \\ \dot{x}_2 &= f(x_2, y_2) + \alpha h(x_8, x_2) + \gamma h(x_1, x_2) \\ \dot{y}_2 &= g(x_2, y_2) + \beta h(y_8, y_2) + \delta h(y_1, y_2). \end{aligned}$$

The dynamics of the ith cell in the quadruped network with nearest neighbor coupling is given by

$$\begin{aligned} \dot{x}_i &= f(x_i, y_i) + \alpha h(x_{i-2}, x_i) + \gamma h(x_{i+\epsilon_i}, x_i) \\ \dot{y}_i &= g(x_i, y_i) + \beta h(y_{i-2}, y_i) + \delta h(x_{i+\epsilon_i}, x_i), \end{aligned} \tag{4.3}$$

where the indices are taken modulo 8 and $\epsilon_i = (-1)^{i+1}$.

We now state the theorem of existence of primary gaits except pronk. In order to prove the existence of a trot with linear synaptic coupling, we need to add extra couplings to the cell system. A bilateral coupling between cell 1 and cell 5 is necessary, and thus the group orbit of connections follows: cell 3 with cell 7, cell 2 with cell 6, and cell 4 with cell 8. Then the coupled cell system (4.3) with linear

synaptic coupling becomes

$$\begin{aligned} \dot{x}_i &= f(x_i, y_i) + \alpha x_{i-2} + \gamma x_{i+\epsilon_i} + \xi x_{i+4} \\ \dot{y}_i &= g(x_i, y_i) + \beta y_{i-2} + \delta x_{i+\epsilon_i} + \eta y_{i+4} \end{aligned} \tag{4.4}$$

Theorem 4.1. *Consider cell system (4.4). Let* $(x_i, y_i) = (x_0, y_0)$ *for all* i *be a stand equilibrium and let* L_0 *be the Jacobian matrix of (4.2) at* (x_0, y_0)*. Suppose that*

$$L_0 \text{ has nonreal eigenvalues.} \tag{4.5}$$

Then by varying coupling parameters only, we can find a Hopf bifurcation from a stand equilibrium to each of pace, bound, trot, walk, and jump primary gaits.

The proof of Theorem 4.1 fails for trot (when second nearest neighbor coupling is not present) and for pronk. However, we have found both trot (without second nearest neighbor coupling) and pronk in the network by numerical simulation. See Section 6.

Since the coupling functions are linear, the nonlinearities of the cell system are independent of the coupling parameters. Therefore, by assuming conditions just on the quadratic and cubic nonlinearities we can assure that all Hopf bifurcations from stand equilibria are supercritical.

We now discuss the stability of primary gaits produced from stand by Hopf bifurcation. To show asymptotic stability of primary gaits at Hopf bifurcation, we need to show that all noncritical eigenvalues have negative real parts. We say that a Hopf bifurcation is *stable* if the critical eigenvalues of the linearization are simple and all other other eigenvalues have negative real part. Using this definition we state our second theorem.

Theorem 4.2. *Consider cell system (4.4). Restrict the coupling parameters by setting* $\delta = \gamma$ *and* $\xi = \eta = 0$*. Assume that a Hopf bifurcation from stand to a periodic solution occurs at coupling parameters* $(\alpha_0, \beta_0, \gamma_0)$*.*

Suppose that $\alpha_0 = \beta_0$*. Then, the Hopf bifurcation for*

(a) a pronk is stable if $\alpha_0 > 0, \gamma_0 > 0$*;*
(b) a pace is stable if $\alpha_0 > 0, \gamma_0 < 0$*;*
(c) a bound is stable if $\alpha_0 < 0, \gamma_0 > 0$*;*
(d) a trot is stable if $\alpha_0 < 0, \gamma_0 < 0$*.*

Suppose that $\alpha_0 = -\beta_0$*. Then, the Hopf bifurcation for*

(e) a jump is stable if $\gamma_0 > 0$*;*
(f) a walk is stable if $\gamma_0 < 0$*.*

The proof of Theorem 4.2 is found in Section 5.3. We note that when $\alpha_0 = \pm\beta_0$, the listed constraints on Hopf bifurcation are both necessary and sufficient. Theorem 4.2 remains valid if $|\alpha - \beta|$ and $|\gamma - \delta|$ are nonzero and small. Then, the conditions for asymptotic stability depend on the sign of the sum of the coupling parameters. For instance, a trot is asymptotically stable if $\alpha + \beta < 0$ and $\gamma + \delta < 0$.

We say that the coupling is *excitatory* if the sum of the coupling parameters is positive, and *inhibitory* if the sum of coupling parameters is negative. Note that in

Theorem 4.2, excitatory coupling at the point of Hopf bifurcation leads to solutions with in-phase output signals and inhibitory coupling leads to output signals with half-period phase shifts. This agrees with the often encountered result that excitatory coupling leads to stable synchronization of oscillators and inhibitory coupling to stable half-period phase shift (or anti-phase) oscillations. See [19] p. 1218 for biological examples, and [33] or [11] for mathematical examples. The quarter-period phase shift along the $\mathbf{Z}_4$ rings of cells needed for the walk and jump solutions is achieved through *neutral* coupling: $\alpha + \beta = 0$.

Our final result states when stable Hopf bifurcations are known to exist.

Theorem 4.3. *In (4.2) assume*

$$(x_0, y_0) \text{ is a spiral sink.} \tag{4.6}$$

If (4.4) has linear synaptic coupling, then there exists coupling parameters leading to a stable Hopf bifurcation for bound, pace, and trot.

The proof proceeds by finding parameter values as in the hypotheses of Theorem 4.1 where Hopf bifurcation actually exists. For walk and jump, the Hopf bifurcation points of Theorem 4.1 do not seem to lead to asymptotically stable periodic solutions and we have not been able to prove a result similar to Theorem 4.3. The difficulty in finding asymptotically stable walk and jump by Hopf bifurcation is based on the fact that stand equilibria move in phase space as coupling parameters are varied. Hence, finding the location of Hopf bifurcation points leading to a stable walk and jump requires the use of numerical approximations or path following software such as AUTO. These gaits can be found by numerical simulation of the cell system equations. See Section 6.

5. Proof of existence and stability theorems

In this section, we prove the existence and stability results stated in Section 4. To prove these results, we need to compute the eigenvalues of the linearization of the system of equations of the network at a stand equilibrium. In the first subsection, we show how a stand equilibrium depends on the coupling parameters. The second subsection is devoted to the computation of the eigenvalues at the stand and the third subsection is devoted to the proofs of the results stated in Section 4.

5.1. The stand equilibrium

A *stand* is an equilibrium that is fixed by all symmetries of the network. Next we consider how stand equilibria depend on parameters. Let (x_0, y_0) be an equilibrium of (4.2).

Proposition 5.1. *Assume (4.5) is valid and the coupling is linear synaptic. There exists a family of stand equilibria parametrized by the coupling parameters:*

$$(x_0(\alpha, \beta, \gamma, \delta, \xi, \eta), y_0(\alpha, \beta, \gamma, \delta, \xi, \eta)),$$

for $(\alpha, \beta, \gamma, \delta, \xi, \eta)$ *in a neighborhood of the origin in* $\mathbf{R}^4$.

Proof. Finding equilibria of the coupled cell system requires solving 16 nonlinear equations. However, at a stand equilibrium, where the cells are all equal, the equations decouple into eight identical systems of two equations. This system is:

$$\begin{aligned} \dot{x} &= f(x, y) + (\alpha + \gamma + \xi)x = 0 \\ \dot{y} &= g(x, y) + (\beta + \delta + \eta)y = 0. \end{aligned} \tag{5.1}$$

We apply the implicit function theorem to (5.1) as follows. The linearization (with respect to the state variables x and y) is $L_0 + A$ where L_0 has nonzero eigenvalues by (4.5) and A has entries near zero. Therefore, $L_0 + A$ has nonzero eigenvalues and the implicit function theorem allows us to solve for x and y in terms of $\alpha, \beta, \gamma, \delta$. □

5.2. Eigenvalues of the linearization at the stand

We compute the eigenvalues of the linearization L of system (4.3) and (4.4) at the stand equilibrium. In particular, we are interested in the real part of the eigenvalues. We take advantage of the isotypic decomposition of the complexified phase space $(\mathbf{C}^8)^2$ to compute the diagonal block structure of L. Let

$$A = \begin{bmatrix} a & b \\ c & d \end{bmatrix}, \quad B = \begin{bmatrix} \alpha & 0 \\ 0 & \beta \end{bmatrix}, \quad C = \begin{bmatrix} \gamma & 0 \\ 0 & \delta \end{bmatrix}, \quad D = \begin{bmatrix} \xi & 0 \\ 0 & \eta \end{bmatrix}.$$

Equation (4.4) has the linearization

$$L = \begin{bmatrix} A & C & 0 & 0 & D & 0 & B & 0 \\ C & A & 0 & 0 & 0 & D & 0 & B \\ B & 0 & A & C & 0 & 0 & D & 0 \\ 0 & B & C & A & 0 & 0 & 0 & D \\ D & 0 & B & 0 & A & C & 0 & 0 \\ 0 & D & 0 & B & C & A & 0 & 0 \\ 0 & 0 & D & 0 & B & 0 & A & C \\ 0 & 0 & 0 & D & 0 & B & C & A \end{bmatrix}. \tag{5.2}$$

The action of $\mathbf{Z}_4 \times \mathbf{Z}_2$ on phase space permutes the indices of the cells. Therefore, the phase space $(\mathbf{R}^8)^2$ consists of two copies of the irreducible representations of $\mathbf{R}^8$. The decomposition of $\mathbf{R}^8$ into irreducible representations is computed in detail in [15] and [4]. Let

$$v_{jk} = (1, (-1)^k, i^j, (-1)^k i^j, i^{2j}, (-1)^k i^{2j}, i^{3j}, (-1)^k i^{3j}).$$

The complex irreducible representations of the action of $\mathbf{Z}_4 \times \mathbf{Z}_2$ on $\mathbf{C}^8$ are $V_{jk} = \mathbf{C}\{v_{jk}\}$, $j = 0, 1, 2, 3$ and $k = 0, 1$. The real irreducible representations are $U_{jk} = V_{jk}$ for $j = 0, 2$ and $k = 0, 1$, $U_{10} = \mathrm{Re}(V_{10} \oplus V_{30})$, and $U_{11} = \mathrm{Re}(V_{11} \oplus V_{31})$. Bases for the irreducible representations U_{ij} and the correspondence of these representations to primary gaits is given in Table 5.

Table 5. Quadrupedal gaits. In jump and walk choose either + or − throughout.

U_{00}	U_{01}	U_{10}	U_{11}	U_{20}	U_{21}
0 0	$0\ \frac{1}{2}$	$\pm\frac{3}{4}\ \pm\frac{3}{4}$	$\pm\frac{3}{4}\ \pm\frac{1}{4}$	$\frac{1}{2}\ \frac{1}{2}$	$\frac{1}{2}\ 0$
0 0	$0\ \frac{1}{2}$	$\frac{1}{2}\ \ \frac{1}{2}$	$\frac{1}{2}\ \ 0$	0 0	$0\ \frac{1}{2}$
0 0	$0\ \frac{1}{2}$	$\pm\frac{1}{4}\ \pm\frac{1}{4}$	$\pm\frac{1}{4}\ \pm\frac{3}{4}$	$\frac{1}{2}\ \frac{1}{2}$	$\frac{1}{2}\ 0$
0 0	$0\ \frac{1}{2}$	$0\ \ 0$	$0\ \ \frac{1}{2}$	0 0	$0\ \frac{1}{2}$
pronk	pace	jump$^{\pm}$	walk$^{\pm}$	bound	trot

The linearization leaves the isotypic components invariant, see Theorem 3.5, Chapter XII [17]. Since the irreducible representations V_{jk} are nonisomorphic, there is a basis where the linearization L decomposes in 2×2 complex diagonal blocks L_{jk}. We find the diagonal blocks by multiplying each eigenvector v_{jk} from the left by L. Table 6 lists the diagonal blocks. The diagonal blocks L_{jk} where $j = 0, 2$ and $k = 0, 1$ are real. The remaining diagonal blocks are complex.

The eigenvalues of the real diagonal blocks are easily computed from the trace and the determinant. The trace of the real diagonal blocks is listed in Table 7. Let $D_{jk} = (\operatorname{tr} L_{jk})^2 - 4 \det L_{jk}$. The value of D_{jk} for the real diagonal blocks is listed in Table 8.

The eigenvalues of the complex diagonal blocks are the same as the eigenvalues of the restriction of the linearization to the real irreducible representations U_{10} and U_{11}.

Table 6. Diagonal blocks of L when coupling is linear synaptic.

Diagonal Blocks (real)	Diagonal blocks (complex)
$L_{00} = A + (B + C + D)$	$L_{10} = A - Bi + C - D$
$L_{01} = A + (B - C + D)$	$L_{11} = A - Bi - C - D$
$L_{20} = A - (B - C - D)$	$L_{30} = A + Bi + C - D$
$L_{21} = A - (B + C - D)$	$L_{31} = A + Bi - C - D$

Table 7. Trace for the real diagonal blocks.

Block	Synaptic: $\operatorname{tr} L_{jk}$
L_{00}	$(a + d) + (\alpha + \beta) + (\gamma + \delta) + (\xi + \eta)$
L_{01}	$(a + d) + (\alpha + \beta) - (\gamma + \delta) + (\xi + \eta)$
L_{20}	$(a + d) - (\alpha + \beta) + (\gamma + \delta) + (\xi + \eta)$
L_{21}	$(a + d) - (\alpha + \beta) - (\gamma + \delta) - (\xi + \eta)$

Table 8. D_{jk} for the real diagonal blocks.

Block	Synaptic: D_{jk}
L_{00}	$((a-d)+(\alpha-\beta)+(\gamma-\delta)+(\xi-\eta))^2+4bc$
L_{01}	$((a-d)+(\alpha-\beta)-(\gamma-\delta)+(\xi-\eta))^2+4bc$
L_{20}	$((a-d)-(\alpha-\beta)+(\gamma-\delta)+(\xi-\eta))^2+4bc$
L_{21}	$((a-d)-(\alpha-\beta)-(\gamma-\delta)+(\xi-\eta))^2+4bc$

The eigenvalues of the complex blocks L_{jk} are also determined by the trace and determinant of the matrix. However, because the matrices are complex, the complex eigenvalues need not be complex conjugates. We want to find an expression for the eigenvalues of complex L_{jk} in the form $u+iv$, where $u, v \in \mathbf{R}$.

The eigenvalues of L_{jk} are given by

$$\frac{1}{2}\left[\operatorname{tr} L_{jk} \pm \sqrt{\left(\operatorname{tr} L_{jk}\right)^2 - 4\det\ L_{jk}}\right].$$

Write $\left(\operatorname{tr} L_{jk}\right)^2 - 4\det\ L_{jk} = \Phi_{jk} + i\Psi_{jk}$. Then,

$$\sqrt{\Phi_{jk}+i\Psi_{jk}} = \frac{1}{\sqrt{2}}\left[\Phi_{jk} + (\Phi_{jk}^2+\Psi_{jk}^2)^{1/2}\right]^{1/2} + \frac{i}{\sqrt{2}}\left[-\Phi_{jk} + (\Phi_{jk}^2+\Psi_{jk}^2)^{1/2}\right]^{1/2}. \tag{5.3}$$

Proposition 5.2. *Let $\Lambda_{jk} = \Phi_{jk}^2 + \Psi_{jk}^2$ and $\tau_{jk} = Re\,(tr\, L_{jk})$. The real part of the eigenvalues of the diagonal block corresponding to the U_{1k}^2 isotypic component are:*

$$\left(\tau_{jk} + \frac{1}{\sqrt{2}}\left[\Phi_{1k} + \Lambda_{1k}^{1/2}\right]^{1/2}\right), \tag{5.4}$$

$$\left(\tau_{jk} - \frac{1}{\sqrt{2}}\left[\Phi_{3k} + \Lambda_{3k}^{1/2}\right]^{1/2}\right) \tag{5.5}$$

Proof. Just add the real part of the trace of L_{jk} to the real part of (5.3) in each case. □

Let $\nu = \operatorname{tr} A$, $\Delta = \det\ A$ and $\mathcal{K} = (\alpha-\beta+\gamma-\delta)^2 - 2(a-d)(\alpha-\beta+\gamma-\delta)$. The expressions Φ_{jk} and Ψ_{jk} are found in Table 9 and Table 10 respectively. The derivation of Φ_{jk} and Ψ_{jk} is routine, see Buono [4] for details.

Remark 5.3. *From Tables 9 and 10, $\Phi_{10} = \Phi_{30}$, $\Phi_{11} = \Phi_{31}$, $\Psi_{10} = -\Psi_{30}$ and $\Psi_{11} = -\Psi_{31}$. Since Ψ_{jk} are squared in Λ_{jk} We write the eigenvalues in Theorem 5.2 using only Φ_{10}, Ψ_{10}, Φ_{11} and Ψ_{11}.*

Corollary 5.4. *For both isotypic components U_{10}^2 and U_{11}^2, there is a pair of complex conjugate eigenvalues for which the real part is always larger than the real part of the other pair of complex conjugate eigenvalues.*

Proof. From Remark 5.3, since $\left(\Phi_{1k} + \Lambda_{1k}^{1/2}\right)^{1/2} = \left(\Phi_{3k} + \Lambda_{3k}^{1/2}\right)^{1/2} > 0$. Then, (5.4) is always greater than (5.5). □

5.3. Proof of Theorems

In this subsection we prove the three results of Section 4. We begin by proving Theorem 4.1. We then explain the limitations of the proof in the pronk case and the trot case without second nearest neighbor coupling. Theorem 4.2 is proved through Proposition 5.5 and Proposition 5.7. Finally, using Theorem 4.2 and Lemma 5.8 we prove Theorem 4.3.

The difficulty of the proof of Theorem 4.1 lies in the fact that in general the stand equilibrium depends on the coupling parameters. In principle this dependence makes it hard to follow the location of the stand and hence its linearization. The idea of the proof is to restrict the coupling parameters in such a way that the stand is independent of the remaining coupling parameters.

We use the following simplifications of the eigenvalues at the stand in the proof of Theorem 4.1. A consequence of (4.5) is that $\nu^2 - 4\Delta < 0$ at (x_0, y_0) and thus remains negative in a neighborhood of the origin in coupling parameter space. Set $\alpha = \beta$, $\gamma = \delta$ and $\xi = \eta$. Then the eigenvalues become simpler. In particular, $D_{jk} = \nu^2 - 4\Delta$ for the real diagonal blocks, see Table 8. Hence the real diagonal blocks have complex conjugate eigenvalues. Moreover, $\Phi_{jk} = \nu^2 - 4\Delta$, and $\Psi_{jk} = 0$, see Table 9 and Table 10 respectively. Hence, this implies that

$$\Phi_{jk} + (\Phi_{jk}^2 + \Psi_{jk}^2)^{1/2} = 0.$$

We note the real part of the eigenvalue with eigenspace U_{jk} by σ_{jk}. Table 11 shows the real part of the eigenvalues when $\alpha = \beta$, $\gamma = \delta$, and $\xi = \eta$.

Table 9. Values of Φ_{jk}.

Blocks	Φ_{jk}: synaptic
L_{10}, L_{30}	$\nu^2 - 4\Delta - (\alpha-\beta)^2 + [(\gamma-\delta) - (\xi-\eta)][2(a-d) + (\gamma-\delta) - (\xi-\eta)]$
L_{11}, L_{31}	$\nu^2 - 4\Delta - (\alpha-\beta)^2 + [(\gamma-\delta) + (\xi-\eta)][(\gamma-\delta) + (\xi-\eta) - 2(a-d)]$

Table 10. Values of Ψ_{jk}.

Blocks	Ψ_{jk}: synaptic
L_{10}	$-2(\alpha-\beta)[(a-d) + (\gamma-\delta) - (\xi-\eta)]$
L_{30}	$2(\alpha-\beta)[(a-d) + (\gamma-\delta) - (\xi-\eta)]$
L_{11}	$-2(\alpha-\beta)[(a-d) - (\gamma-\delta) - (\xi-\eta)]$
L_{31}	$2(\alpha-\beta)[(a-d) - (\gamma-\delta) - (\xi-\eta)]$

Table 11. Real part of eigenvalues when $\alpha = \beta$, $\gamma = \delta$, and $\xi = \eta$: synaptic case.

Block	Real part of eigenvalue	Block	Real part of eigenvalue
L_{00}	$\sigma_{00} = \nu + 2(\alpha + \gamma + \xi)$	L_{21}	$\sigma_{21} = \nu - 2(\alpha + \gamma - \xi)$
L_{01}	$\sigma_{01} = \nu + 2(\alpha - \gamma + \xi)$	L_{10}	$\sigma_{10} = \nu + 2\gamma - 2\xi$
L_{20}	$\sigma_{20} = \nu + 2(-\alpha + \gamma + \xi)$	L_{11}	$\sigma_{11} = \nu - 2\gamma - 2\xi$

Proof of Theorem 4.1. Consider the walk. The pace, bound and jump are done in a similar way. For these cases, we can assume that $\xi = \eta = 0$. We work the trot case below. Let $\alpha = \beta$ and $\gamma = \delta$, then $\sigma_{11} = \nu - 2\gamma$. Let $\nu_0 = \nu|_{(x_0, y_0)}$ and $\alpha = -\gamma$, then $(x, y, \gamma) = (x_0, y_0, \nu_0/2)$ is a solution to the system of equations

$$\begin{cases} F(x, y, \alpha, \gamma) = f(x, y) + (\alpha + \gamma)x = 0 \\ G(x, y, \alpha, \gamma) = g(x, y) + (\alpha + \gamma)y = 0 \\ E(x, y, \alpha, \gamma) = \nu - 2\gamma = 0. \end{cases}$$

At $(x_0, y_0, \nu_0/2)$, the linearization at the stand equilibrium has a pair of purely imaginary eigenvalues with eigenspace U_{11}. The eigenvalues cross the imaginary axis at speed $E_\gamma(x_0, y_0, \nu_0/2) = -2 \neq 0$ since ν does not depend on γ when $\alpha = -\gamma$. Thus, a Hopf bifurcation to walk occurs. See Table 5 where the correspondence of U_{11} to walk is shown.

We can go a little bit further. Note that the determinant of

$$\left.\frac{\partial(F, G, E)}{\partial(x, y, \gamma)}\right|_{(x_0, y_0, -\nu_0/2, \nu_0/2)} = \begin{bmatrix} \frac{\partial f}{\partial x}(x_0, y_0) & \frac{\partial f}{\partial y}(x_0, y_0) & x_0 \\ \frac{\partial g}{\partial x}(x_0, y_0) & \frac{\partial g}{\partial y}(x_0, y_0) & y_0 \\ \frac{\partial \nu}{\partial x}(x_0, y_0) & \frac{\partial \nu}{\partial y}(x_0, y_0) & -2 \end{bmatrix} \tag{5.6}$$

is generically nonzero since $\frac{\partial f}{\partial x}(x_0, y_0)\frac{\partial g}{\partial y}(x_0, y_0) - \frac{\partial f}{\partial y}(x_0, y_0)\frac{\partial g}{\partial x}(x_0, y_0)$ is nonzero. Hence, by the implicit function theorem $(x(\alpha), y(\alpha), \alpha, \gamma(\alpha))$ is a solution to $F = G = E = 0$ for all values of α in a neighborhood of $\nu_0/2$. Moreover, for a possibly smaller neighborhood around $\nu_0/2$ the nonzero speed crossing condition is satisfied on the branch parametrized by α. Thus, we have proved that if the determinant of (5.6) is nonzero, there exists a branch of Hopf bifurcation leading to walk.

In the trot case, we let ξ and η be different from zero. Set $\eta = \xi$. We solve the system

$$\begin{cases} F(x, y, \alpha + \gamma, \xi) = f(x, y) + (\alpha + \gamma + \xi)x = 0 \\ G(x, y, \alpha + \gamma, \xi) = g(x, y) + (\alpha + \gamma + \xi) = 0 \\ E(x, y, \alpha + \gamma, \xi) = \nu - 2(\alpha + \gamma) + 2\xi = 0. \end{cases} \tag{5.7}$$

restricted to the subspace $\alpha+\gamma+\xi=0$. A solution to this system is at $(x, y, \alpha+\gamma, \xi)=(x_0, y_0, -\nu_0/4, \nu_0/4)$, so the linearization at the stand has a pair of imaginary eigenvalues with eigenspace U_{21}. (See Table 5 for the relationship of U_{21} to trot.) The eigenvalues cross the imaginary axis with speed $E_\xi(x_0, y_0, -\nu_0/4, \nu_0/4) = 2 \neq 0$ since ν is constant on $\alpha+\gamma=-\xi$. We remove the restriction that $\xi=-(\alpha+\gamma)$. As above, the determinant of

$$\left.\frac{\partial(F, G, E)}{\partial(x, y, \xi)}\right|_{(x_0, y_0, -\nu_0/4, \nu_0/4)} = \begin{bmatrix} \frac{\partial f}{\partial x}(x_0, y_0) & \frac{\partial f}{\partial y}(x_0, y_0) & x_0 \\ \frac{\partial g}{\partial x}(x_0, y_0) & \frac{\partial g}{\partial y}(x_0, y_0) & y_0 \\ \frac{\partial \nu}{\partial x}(x_0, y_0) & \frac{\partial \nu}{\partial y}(x_0, y_0) & 2 \end{bmatrix}$$

is generically nonzero. Hence, by the implicit function theorem $(x(\alpha+\gamma), y(\alpha+\gamma), \xi(\alpha+\gamma))$ is a solution to $F=G=E=0$ for all values of $\alpha+\gamma$ in a neighborhood of $-\nu_0/4$. Moreover, for a possibly smaller neighborhood around $-\nu_0/4$ the nonzero speed crossing condition is satisfied on the branch parametrized by $\alpha+\gamma$. □

Under assumption (4.5), the existence of trot without the second nearest neighbor coupling and of pronk cannot be proved. Consider the case of trot. To obtain a Hopf bifurcation from stand to trot we solve the following system.

$$\begin{aligned} f(x, y)+(\alpha+\gamma)x &= 0 \\ g(x, y)+(\beta+\delta)y &= 0 \\ \sigma_{21}=\nu-(\alpha+\gamma)-(\beta+\delta) &= 0. \end{aligned} \tag{5.8}$$

By setting $\alpha+\gamma=\beta+\delta=0$, (x_0, y_0) is a solution to $f(x, y)=g(x, y)=0$. Then $\sigma_{21}=0$ if and only if $\nu_0=0$. However, from (4.5), ν_0 is not necessarily equal to zero. Now, if we let either $\alpha+\gamma$ or $\beta+\delta$ be different from zero, then the existence of a stand solution for the system is not guaranteed anymore.

The same explanation is valid in the pronk case. Moreover, the existence of pronk cannot be shown by adding extra connections in the network. When adding an extra connection in the network, we find stand by solving

$$\begin{aligned} f(x, y)+(\alpha+\gamma+\mu)x &= 0 \\ g(x, y)+(\beta+\delta+\rho)y &= 0 \end{aligned}$$

where μ and ρ are the coupling parameters for the new connection. We multiply the linearization L, see (5.2), by the eigenvector v_{00}. Then the trace of the diagonal block L_{00} is $\nu+(\alpha+\beta+\gamma+\delta+\mu+\rho)$ and it corresponds to the real part of the eigenvalue of L_{00}. Hence, the same obstruction as was shown above occurs.

We now turn to the proof of the stability result. Note that for diagonal blocks L_{10} and L_{11}, we always refer to the real part of the eigenvalue with greatest real part, see Corollary 5.4.

Let $\mathscr{P}_{jk}$ be the periodic solution produced from Hopf bifurcation with eigenspace contained in U_{jk}^2.

Proposition 5.5. *Let $\alpha = \beta$, $\gamma = \delta$, and $\xi = \eta = 0$ in network (4.4). Suppose that a Hopf bifurcation from stand occurs for (α_0, γ_0) to a periodic solution $\mathscr{P}$. Consider the following statement:*

$$sgn\,\gamma_0 = (-1)^k \quad and \quad \alpha_0 = \begin{cases} +1 \text{ if } j = 0 \\ -1 \text{ if } j = 2. \end{cases} \tag{5.9}$$

Suppose that $\mathscr{P} = \mathscr{P}_{jk}$. Then $\mathscr{P}$ is asymptotically stable if and only if (5.9) holds.

Proof. We show the theorem in the L_{21} case; that is, a trot periodic solution bifurcates. A trot bifurcates when $\sigma_{21} = 0$, that is $\nu = 2(\alpha + \gamma)$. We substitute ν in σ_{jk}, $(j, k) \neq (2, 1)$. Then, $\sigma_{00} = 4(\alpha + \gamma)$, $\sigma_{01} = 4\alpha$, $\sigma_{20} = 4\gamma$, $\sigma_{10} = 2\alpha + 4\gamma$ and $\sigma_{11} = 2\alpha$. So, all noncritical eigenvalues at the Hopf bifurcation have negative real parts if and only if $\alpha < 0$ and $\gamma < 0$. The proof for the other gaits is done in a similar way. □

Proposition 5.6. *Let $\alpha = \beta \neq 0$, $\gamma = \delta$, and $\xi = \eta = 0$ be fixed in network (4.4). Suppose that either matrix L_{10} or L_{11} has a simple imaginary eigenvalue, then at least one eigenvalue has a positive real part.*

Proof. If $\nu = 2\gamma$, then $\sigma_{10} = 0$. So, $\sigma_{01} = 2\alpha$ and $\sigma_{21} = -2\alpha$. Thus, for any value of $\alpha \neq 0$, one of the real parts is positive. A similar argument shows the L_{11} case. □

Consider now the diagonal blocks L_{10} and L_{11}. Let $\beta = -\alpha$ and $\gamma = \delta$. If we choose $\alpha \neq 0$ small enough, then σ_{jk} for the real blocks is given by the trace: $\sigma_{00} = \sigma_{20} = \nu + 2\gamma$ and $\sigma_{01} = \sigma_{21} = \nu - 2\gamma$. When $\gamma = \delta$, $\Phi_{10} = \Phi_{11} = \Phi$ and $\Psi_{10} = \Psi_{11} = \Psi$, then $\sigma_{10} = \nu + 2\gamma + \frac{1}{\sqrt{2}}(\Phi + (\Phi^2 + \Psi^2)^{1/2})^{1/2}$ and $\sigma_{11} = \nu - 2\gamma + \frac{1}{\sqrt{2}}(\Phi + (\Phi^2 + \Psi^2)^{1/2})^{1/2}$.

Proposition 5.7. *Let $\alpha = -\beta$, $\gamma = \delta$, and $\xi = \eta = 0$ in network (4.4). Suppose that a Hopf bifurcation from stand occurs for (α_0, γ_0) to a periodic solution $\mathscr{P}$. Suppose that $\mathscr{P} = \mathscr{P}_{1k}$. Then $\mathscr{P}$ is asymptotically stable if and only if $sgn\,\gamma_0 = (-1)^k$.*

Proof. Solve $\sigma_{10} = 0$ by isolating ν:

$$\nu = -2\gamma - \frac{1}{\sqrt{2}}(\Phi + (\Phi^2 + \Psi^2)^{1/2})^{1/2}. \tag{5.10}$$

Replace ν in σ_{11}, σ_{00}, and σ_{01}, respectively. After simplification we obtain -4γ, $-\frac{1}{\sqrt{2}}(\Phi + (\Phi^2 + \Psi^2)^{1/2})^{1/2}$, and $-4\gamma - \frac{1}{\sqrt{2}}(\Phi + (\Phi^2 + \Psi^2)^{1/2})^{1/2}$. It is easy to see that these three quantities are negative if and only if $\gamma > 0$. Solve $\sigma_{11} = 0$ for ν:

$$\nu = 2\gamma - \frac{1}{\sqrt{2}}(\Phi + (\Phi^2 + \Psi^2)^{1/2})^{1/2}. \tag{5.11}$$

Replace ν in σ_{10}, σ_{00}, and σ_{01}, respectively. After simplification we obtain 4γ, $4\gamma - \frac{1}{\sqrt{2}}(\Phi + (\Phi^2 + \Psi^2)^{1/2})^{1/2}$, and $-\frac{1}{\sqrt{2}}(\Phi + (\Phi^2 + \Psi^2)^{1/2})^{1/2}$. It is easy to

see that $-\frac{1}{\sqrt{2}}(\Phi + (\Phi^2 + \Psi^2)^{1/2})^{1/2}$ is always negative and that 4γ is negative if and only if $\gamma < 0$. Therefore, $4\gamma - \frac{1}{\sqrt{2}}(\Phi + (\Phi^2 + \Psi^2)^{1/2})^{1/2}$ is also negative. □

We need the following lemma for the proof of Theorem 4.3

Lemma 5.8. *Let $\alpha = \beta$, $\gamma = \delta$, and $\xi = \eta$ in (4.4). Suppose that a Hopf bifurcation from stand at $(\alpha_0, \gamma_0, \xi_0)$ leads to a trot periodic solution. Then Hopf bifurcation to trot is stable if and only if $\alpha_0 < 0$, $\gamma_0 < 0$, and $\xi_0 > \alpha_0/2$.*

Proof. Trot is found on the subspace $\xi = -(\alpha + \gamma)$. Solving $\sigma_{21} = 0$ we obtain $\nu_0 = 2\alpha + 2\gamma - \xi$. Replacing in σ_{jk} for $(j, k) \neq (2, 1)$, we obtain $\sigma_{00} = 4(\alpha + \gamma)$, $\sigma_{10} = 4\alpha$, $\sigma_{20} = 4\gamma$, $\sigma_{11} = 2\alpha - 4\xi$, and $\sigma_{10} = 2\alpha + 4\gamma - 4\xi$. Now, $\sigma_{00} < 0$, $\sigma_{10} < 0$, and $\sigma_{20} < 0$ if and only if $\alpha < 0$ and $\gamma < 0$. Thus $\xi = -(\alpha + \gamma) > 0$, and therefore, σ_{11} and σ_{10} are also negative. □

Proof of Theorem 4.3. We assume $\gamma = -\alpha$ to find pace and bound. On that subspace the stand equilibrium does not move and so $\nu = \nu_0$. Now $\sigma_{01} = 0$ if and only if $\alpha_0 = -\nu_0/4$. Since the cell dynamics satisfies (4.6), then $\alpha_0 > 0$, and $\gamma_0 = -\alpha_0 < 0$. From Theorem 4.2 the Hopf bifurcation to pace is stable. Now, $\sigma_{20} = 0$ if and only if $\alpha_0 = \nu_0/4$. Similarly, since the cell dynamics satisfies (4.6), $\alpha_0 < 0$ and $\gamma_0 > 0$. From Theorem 4.2, the Hopf bifurcation to bound is stable.

We solve σ_{21} when $\xi = -(\alpha + \gamma)$ by setting $\xi_0 = -\nu_0/4 > 0$. Since $\nu_0 < 0$ by (4.6), take $\alpha_0 < 0$ and $\gamma_0 < 0$ such that $-(\alpha_0 + \gamma_0) = -\nu_0/4$. Since $\xi_0 > 0$, by Lemma 5.8 the Hopf bifurcation to trot is stable. □

6. Numerical simulations

Numerical simulations are performed using the dimensionless Morris-Lecar equations [34, 30] as cell dynamics:

$$\begin{aligned} \dot{v} &= -g_{Ca} m(v)(v-1) - g_l(v - v_l) - g_K w(v - v_K) + i \equiv f(u, v) \\ \dot{w} &= \phi\tau(v)(n(v) - w) \qquad\qquad\qquad\qquad\qquad\quad \equiv g(u, v) \end{aligned}$$

where

$$m(v) = \tfrac{1}{2}\left(1 + \tanh\left(\frac{v - v_1}{v_2}\right)\right)$$

$$n(v) = \tfrac{1}{2}\left(1 + \tanh\left(\frac{v - v_3}{v_4}\right)\right)$$

$$\tau(v) = \cosh\left(\frac{v - v_3}{2v_4}\right)$$

Using the results of the previous section we can locate Hopf bifurcation points leading to stable primary gaits. Hypothesis (4.6) is satisfied for the following parameter values of the Morris-Lecar equations: $\phi = 0.2$, $v_1 = 0.2$, $v_2 = 0.4$, $v_3 = 0.3$, $v_4 = 0.2$, $g_{Ca} = 3$, $g_l = 0.6$, $g_K = 1.8$, $v_l = -1.8$, $v_K = -0.8$, $i = 1$.

Table 12. Approximate values of synaptic coupling parameters where stable Hopf bifurcations occur.

Gait	$\alpha = \beta$	$\gamma = \delta$	$\xi = \eta$
Pace	0.3	-0.32	0
Bound	-0.32	0.3	0
Trot	0.15	-0.16	-0.31

Table 13. Synaptic coupling parameters where primary gaits are found: $\xi = \eta = 0$.

Gait	α	β	γ	δ	Gait	α	β	γ	δ
Pronk	0.2	0.2	0.2	0.2	Trot	-0.6	-0.6	-0.6	-0.6
Pace	0.2	0.2	-0.2	-0.2	Jump	0.01	-0.01	0.2	0.2
Bound	-0.2	-0.2	0.2	0.2	Walk	0.01	-0.01	-1.2	-1.2

The stand equilibrium is at $(v_0, w_0) \approx (0.31, 0.52)$, and $\nu_0 \approx -1.24$. From the proof of Proposition 4.3, we find parameter values for stable Hopf bifurcation points to pace, bound and trot, see Table 12. The genericity condition in the proof of Theorem 4.1 is easily verified for pace, bound, and trot. Table 13 shows coupling parameter values where primary gaits are observable in numerical simulations. The numerical simulations shown in Figure 2 are the trot and walk periodic solutions for the values in Table 13.

7. Discussion and summary

In this paper, we contribute both to the modeling of central pattern generators for quadruped locomotion by coupled cell systems of differential equations and their analysis.

We contribute to the modeling of quadruped locomotion CPGs by proving that the smallest symmetric network that can model walk, trot and pace as nonconjugate periodic solutions is the $\mathbf{Z}_4 \times \mathbf{Z}_2$ network introduced in [15] (see Theorem 3.2). The proof of this result is based on a general classification theorem for robust periodic solutions in symmetric coupled cell systems (see Theorem 2.2).

One of the main tenets in modeling locomotion CPGs by coupled cell systems is that the signal from each cell is transmitted to precisely one leg. Although the modeling of walk, trot, and pace leads to one eight-cell network whose symmetry group is $\mathbf{Z}_4 \times \mathbf{Z}_2$, it does not lead to a unique choice of assignment of cells to legs. Indeed, many such assignments are possible. However, when we make the additional assumption that symmetries of the network permute pairs of cells that send signals to the same leg, then only two cell to leg assignments are possible (see Theorem 3.3). In [16] we have presented evidence that it is better to think of the signals going from cells to muscle groups (as two muscle groups — flexors and extensors — are needed to control each joint). This interpretation gives a physio-

logical basis for the existence of a doubled-up eight-cell network, as opposed to a simple four-cell network, and makes the assumption on cell to leg assignment seem even more natural.

These two remaining assignments, the zig-zag network and the criss-cross network (see Figure 6), have the property that for primary gaits the cells that send signals to the same leg are either in-phase or a half-period out-of-phase. In the zig-zag network, the cell signals to the same leg are out-of-phase in walk and jump, while the cell signals are in-phase for the remaining primary gaits; in the criss-cross network, the situation is reversed. The evidence for signals being sent to muscle groups in [16] is based on bipeds where there is a distinction between the run (cells in-phase) and walk (cells out-of-phase). This allows a mathematical classification of quadruped gaits as either *walk-like* or *run-like* depending on whether the two signals are out-of-phase or in-phase. It remains to be seen whether there is a corresponding physiological distinction between the walk-like and run-like gaits in quadrupeds. Such a distinction would further confirm the validity of doubled-up networks for modeling locomotion CPGs.

Regarding the analysis of the $\mathbf{Z}_4 \times \mathbf{Z}_2$ network, we have shown (using Hopf equivariant bifurcation theory) that coupling parameters can control the existence and stability of primary gaits by making only mild assumptions on the internal cell dynamics (see Theorems 4.1 and 4.2). Our assumptions are: the cells are two dimensional with an equilibrium having nonreal eigenvalues and the coupling is linear synaptic. These results tell us how to find primary gaits in the network and we do this computationally when using the dimensionless Morris-Lecar equations as internal dynamics. The question of how to find secondary gaits in the $\mathbf{Z}_4 \times \mathbf{Z}_2$ network is addressed in Buono [5].

The structure of our model network (as a symmetric coupled cell system) produces several testable predictions (some of which were outlined in [16]). These predictions include the existence of the jump gait, the physiological differences between primary and secondary gaits, and the physiological differences between walk- and run-like gaits. Moreover, these predictions are consequences of the doubled-up network, which is forced on us simply by trying to model mathematically walk, trot, and pace.

A. Appendix: Symmetry-generated subgroups

We prove Theorem 2.2 by characterizing all symmetry-generated subgroups of Γ-equivariant differential equations (2.1) when $\Gamma \subset \mathbf{O}(n)$ is a finite group and then specializing this result to coupled cell systems. The proof of the general theorem is implicit in the work of Field *et al.* [12].

Let $K \subset H$ be a pair of subgroups of Γ. In addition to (2.2), there are four restrictions imposed on this pair so that a periodic solution $U(t)$ of (2.1) can exist with spatial symmetries K and spatio-temporal symmetries H.

The first restriction is as follows. Suppose that U_0 is any point on this trajectory and suppose that

$$\gamma U_0 = U_0. \tag{A.1}$$

Then, uniqueness of solutions guarantees that $\gamma U(t) = U(t)$ for every t. It follows that $(\gamma, 0)$ is a spatio-temporal symmetry of $U(t)$ and that $\gamma \in K$. The subgroup of Γ consisting of all γ satisfying (A.1) is called the *isotropy subgroup* of U_0. Thus

$$K \text{ is an isotropy subgroup of the action of } \Gamma \text{ on } \mathbf{R}^n. \tag{A.2}$$

The second restriction is straightforward:

$$\dim \mathrm{Fix}(K) \geq 2, \tag{A.3}$$

where

$$\mathrm{Fix}(K) = \{U \in \mathbf{R}^n : \sigma U = U \quad \forall \sigma \in K\} \tag{A.4}$$

is the *fixed-point subspace* of K. By definition a periodic solution with spatial symmetries K must lie in the subspace $\mathrm{Fix}(K)$. Hence the dimension of $\mathrm{Fix}(K)$ must be at least two.

A consequence of the discussion preceding restriction (A.2) is: If $U(0) \in \mathrm{Fix}(\Sigma)$, then the trajectory $U(t)$ must lie in the subspace $\mathrm{Fix}(\Sigma)$ for all t; that is, fixed-point subspaces are flow invariant. Define

$$L_K = \bigcup_{\gamma \notin K} \mathrm{Fix}(\gamma) \cap \mathrm{Fix}(K)$$

Melbourne *et al.* [29] use (a variant of) L_K to restrict the possible symmetry groups of attractors; we now explain how this is done for periodic solutions.

Since K is an isotropy subgroup, L_K is the union of proper subspaces of $\mathrm{Fix}(K)$. More precisely, suppose that $\mathrm{Fix}(\gamma) \supset \mathrm{Fix}(K)$, then the isotropy subgroup of every point in $\mathrm{Fix}(K)$ would contain both K and $\gamma \notin K$. Therefore, the isotropy subgroup of any point in $\mathrm{Fix}(K)$ would be larger than K, and K could not be an isotropy subgroup.

The third restriction placed on symmetry generated subgroups is:

$$H \text{ fixes a connected component of } \mathrm{Fix}(K) - L_K. \tag{A.5}$$

To verify (A.5) we begin by showing that any $\delta \in N(K)$, where $N(K)$ is the normalizer of K in Γ, permutes connected components of $\mathbf{R}^n - L_K$. Observe that

$$\delta(\mathrm{Fix}(\gamma) \cap \mathrm{Fix}(K)) = \mathrm{Fix}(\delta\gamma\delta^{-1}) \cap \mathrm{Fix}(\delta K \delta^{-1}) = \mathrm{Fix}(\delta\gamma\delta^{-1}) \cap \mathrm{Fix}(K)$$

Moreover, $\delta\gamma\delta^{-1} \notin K$. If it were, then γ would be in $\delta^{-1}K\delta = K$, which it is not. Therefore, $\delta : L_K \to L_K$. Since δ is invertible, $\delta : \mathbf{R}^n - L_K \to \mathbf{R}^n - L_K$ and δ permutes the connected components of $\mathbf{R}^n - L_K$.

Since H/K is cyclic, we can choose an element $h \in H$ that projects onto a generator of H/K. Note that $h \in N(K)$ and therefore h permutes the connected components of $\mathbf{R}^n - L_K$. We now show that h (and hence H) must fix one of the connected components. Suppose that the trajectory of $x(t)$ intersects the flow invariant subspace $\mathrm{Fix}(\gamma) \cap \mathrm{Fix}(K)$. Flow invariance of $\mathrm{Fix}(\gamma)$ implies that γ is a spatial symmetry of the solution $x(t)$ and, by definition $\gamma \in K$. Therefore, the trajectory of $x(t)$ does not intersect L_K. Since h is a spatio-temporal symmetry of $x(t)$,

it preserves the trajectory of $x(t)$. Therefore, h must map the connected component of $\mathbf{R}^n - L_K$ that contains the trajectory of $x(t)$ into itself, thus verifying (A.5).

The last restriction occurs when $\dim \mathrm{Fix}(K) = 2$:

$$\text{If } \dim \mathrm{Fix}(K) = 2, \text{ then either } H = K \text{ or } H = N(K). \tag{A.6}$$

A simple example illustrates the difficulty. Suppose that $\Gamma = \mathbf{Z}_4(\rho)$ acting by rotations on $\mathbf{R}^2$, $H = \mathbf{Z}_2(\rho^2)$ and $K = \mathbf{1}$. Observe that $H/K = \mathbf{Z}_2$ is cyclic, K is an isotropy subgroup, $\dim \mathrm{Fix}(K) = 2$, and $L_K = \{0\}$; so all previous restrictions are satisfied. Note, however, that $N(K) = \mathbf{Z}_4$ and hence $N(K) \supsetneq H \supsetneq K$. Finally, suppose that $x(t)$ is a T-periodic solution whose spatio-temporal symmetry is $\rho^2 x(t) = x(t + \frac{T}{2})$. The trajectory of $x(t)$ must avoid the origin and, because ρ^2 is rotation by π, the trajectory must have the origin in its interior. In this case $\rho\{x(t)\}$ must intersect $\{x(t)\}$. Hence $\rho\{x(t)\} = \{x(t)\}$ and $\rho x(t) = x(t \pm \frac{T}{4})$; that is, the spatio-temporal symmetry group is larger than H. In effect, this is the only type of difficulty that can arise, as we now show. Suppose that $H \supsetneq K$; then $H/K = \mathbf{Z}_m$ for some $m \geq 2$. We claim that H/K is generated by a rotation; the only other possibility is that $H/K = \mathbf{Z}_2(\tau)$ where τ acts as a reflection on $\mathrm{Fix}(K)$. Since $\tau\{x(t)\} = \{x(t)\}$ it follows that $\{x(t)\} \cap \mathrm{Fix}(\tau) \neq \emptyset$. Thus $\{x(t)\} \subset \mathrm{Fix}(\tau)$, which is not possible. As in the example, H/K is generated by a rotation. It follows that $L_K = \{0\}$; otherwise, $\mathrm{Fix}(K) - L_K$ has more than one connected component (which must be wedges) and none of these can be fixed by a rotation. As in the example, $x(t)$ must contain the origin in its interior. If $\gamma \in N(K) - H$, then $\gamma\{x(t)\}$ must intersect $\{x(t)\}$ and the spatio-temporal symmetry group of $x(t)$ must be larger than H.

Theorem A.1. *The pair of subgroups $K \subset H$ corresponds to a symmetry generated subgroup if and only if the pair satisfies (2.2), (A.2), (A.3), (A.5), and (A.6). Moreover, asymptotically stable limit cycles with the desired symmetry exist.*

Proof. In the preceding discussion we have proved that the five conditions are necessary; now we prove that they are sufficient. We must prove the existence of a robust periodic solution with space symmetries K and spatio-temporal symmetries H. We sketch that proof here showing, in addition, that the robust periodic solution can be a stable limit cycle.

Choose a generator h of $H/K = \mathbf{Z}_m$. By assumption, H fixes a connected component C of $\mathrm{Fix}(K) - L_K$. Recall that $N(K) \subset \Gamma$ is the largest subgroup that acts on $\mathrm{Fix}(K)$ and that elements in $N(K)$ permute the connected components of $\mathbf{R}^n - L_K$. Define

$$\hat{H} = \{\gamma \in N(K) : \gamma(C) = C\}.$$

Two points need to be verified.

(a) There is a non-self-intersecting closed curve J in C that is mapped onto itself by h and no point on J is fixed by h. Moreover, $\gamma(J) \cap J = \emptyset$ for all $\gamma \in \hat{H} - H$. If so, we can construct a C^∞ vector field f on C for which J is a stable limit cycle and we can smooth f so that it is zero near L_K and near $\gamma(J)$ for all $\gamma \in \hat{H} - H$.

(b) There is a smooth extension of f to all of $\mathbf{R}^n$ that is Γ-equivariant.

Once these points are verified the proof may be completed as follows. Since K is an isotropy subgroup, the space symmetry subgroup of J is K. Since $h : J \to J$, h is a spatio-temporal symmetry of J and the spatio-temporal symmetry group of J is H. Proving that hyperbolic periodic solutions with space symmetries K and spatio-temporal symmetries H are robust (that is, they perturb to periodic solutions with the same symmetry subgroups) is straightforward. Since hyperbolicity implies that the perturbed periodic solution $V(t)$ is unique, it follows that $V(t) \in \mathrm{Fix}(K)$ for all t and that $hV(t)$ must be the same trajectory as $V(t)$. Since the number of temporal symmetries of $U(t)$ is m, it follows by continuity that the spatio-temporal symmetries of $V(t)$ form the subgroup H.

To verify (a) choose a point $x_1 \in C$ and form the group orbit $x_j = h^j x_1$ for $j = 2, \ldots, m$. Note that the points $x_j \in C$ since $h : C \to C$. Choose a non-self-intersecting smooth curve J_1 in C connecting x_1 to x_2, which is possible since C is connected. We can also arrange that near its endpoints J_1 is a straight line in the directions v_1 and v_2, where $(dh)_{x_1}(v_1) \equiv h(v_1) = v_2$. Now let $J = \cup_j h^j(J_1)$. By construction $J \subset C$ is a smooth curve that is invariant under h. There are two difficulties: J can intersect itself and J might intersect $\gamma(J)$ where $\gamma \in \hat{H} - H$. If $\dim \mathrm{Fix}(K) \geq 3$, then we can use transversality arguments (like those used to prove the Whitney embedding theorem, see [14]) to avoid these difficulties in our choice of J. If $\dim \mathrm{Fix}(K) = 2$, then there is a potential problem when constructing J; see Figure 7. Suppose h is rotation by $\frac{4\pi}{5}$, which generates the cyclic group $\mathbf{Z}_5$. Then self intersections of J are unavoidable. If, however, we choose the generator to be $h_* = h^3$ to be rotation through $\frac{2\pi}{5}$, then self intersection can be avoided. So even when $\dim \mathrm{Fix}(K) = 2$ the construction of J is possible. Moreover, when $\dim \mathrm{Fix}(K) = 2$ assumption (A.6) states that either $H = N(K)$ in which case no restrictions come from $\hat{H}$ or $H = K$ in which case we choose a small curve J in $\mathbf{R}^2 - L_K$ that does not intersect any of its images under $N(K)$.

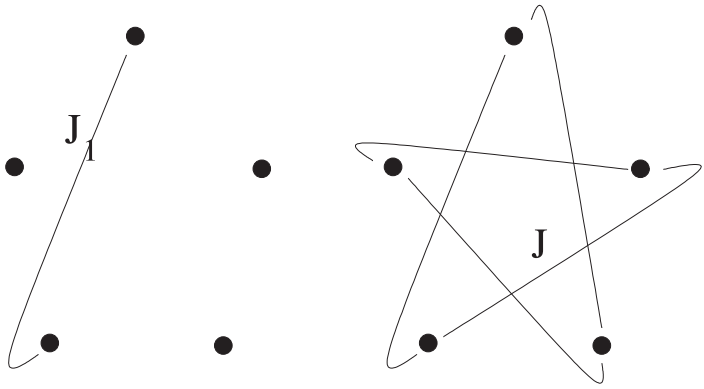

Fig. 7. Unavoidable self intersection in J with certain generators of H/K when $\dim \mathrm{Fix}(K) = 2$.

To verify (b) we average f over the group. First, extend f to $f_1 : \mathrm{Fix}(K) \to \mathrm{Fix}(K)$ by setting $f = 0$ off C. Then let

$$f_2(x) = \frac{1}{|N(K)|} \sum_{\gamma \in N(K)} \gamma^{-1} f(\gamma x).$$

The vector field f_2 is $N(K)$-equivariant, zero near L_K, and has J as a stable limit cycle. Next extend f_2 to $f_3 : \mathbf{R}^n \to \mathbf{R}^n$ so that J is now a stable limit cycle in all of $\mathbf{R}^n$ and $f_3 = 0$ outside a neighborhood of J. In particular, $f_3 = 0$ near L_K. Now average again by setting

$$f_4(x) = \frac{1}{|\Gamma|} \sum_{\gamma \in \Gamma} \gamma^{-1} f_3(\gamma x).$$

The vector field f_4 is the desired extension. □

Remark A.2. Suppose that h is a generator of $\mathbf{Z}_m = H/K$. Is there a periodic solution such that $(h, \frac{1}{m})$ is a spatio-temporal symmetry? The answer may be no when $\dim \mathrm{Fix}(K) = 2$. In this case, we can always choose some generator $h' \in \mathbf{Z}_m = H/K$ so that $(h', \frac{1}{m})$ is a spatio-temporal symmetry; but we can not necessarily choose every generator h.

We now prove Theorem 2.2. Suppose that

$$\dim(\mathrm{Fix}(\gamma) \cap \mathrm{Fix}(K)) \leq \dim \mathrm{Fix}(K) - 2. \tag{A.7}$$

whenever $\gamma \notin K$. Then $\mathrm{Fix}(K) - L_K$ is connected and (A.5) is automatically valid. Therefore, if each irreducible representation of Γ that occurs in the state space $\mathbf{R}^n$ occurs at least twice, then (A.7) is satisfied and (A.5) is valid.

Next we discuss symmetry generated subgroups in coupled cell systems. If the internal dynamics of a coupled cell system is $k \geq 2$, then each irreducible representation appearing in state space appears at least k times. Therefore, in these coupled cell systems, each fixed-point subspace has dimension divisible by k and condition (A.5), and hence (A.7) and (A.3), are satisfied. In particular, since K acts by permuting cells, K divides the set of cells into p blocks where K acts transitively on each block. Moreover, vectors in $\mathrm{Fix}(K)$ have identical components in each block. Therefore, the dimension of $\mathrm{Fix}(K)$ is kp. If $\dim \mathrm{Fix}(K) = 2$, then the internal dynamics in each cell is $k = 2$ dimensional and the number of blocks is $p = 1$. Since Γ acts transitively on the N cells and $|\Gamma| = N$, it follows that the only transitive subgroup is Γ and $K = \Gamma$. Therefore $H = K$ in this case and (A.6) is satisfied.

Finally, suppose that the permutation group Γ has the same number of elements as the number of cells. Then the state space of the coupled cell system consists of k copies of $\mathscr{L}^2(\Gamma)$, the vector space of all real-valued functions on Γ. It is a standard result that all irreducible representations of Γ lie in $\mathscr{L}^2(\Gamma)$. It follows from Barany *et al.* [3] that for these cell systems every subgroup of Γ is an isotropy subgroup, and (A.2) is automatically satisfied. We have proved Theorem 2.2. □

We end this discussion by considering the question of whether robust periodic solutions exist in our coupled cell systems when H/K is cyclic. If all kinds of coupling is permitted consistent with Γ symmetry and arbitrary internal dynamics are allowed, then the coupled cell system is just a general Γ-equivariant vector field. In this generality Theorem A.1 implies that there exist robust periodic solutions for each spatio-temporal symmetry group satisfying (2.2). However, if restrictions are placed on couplings, such as allowing only nearest neighbor coupling or imposing a certain kind of coupling, then Theorem 2.2 does not necessarily guarantee the existence of robust periodic solutions for every possible symmetry generated subgroup. Theorem 2.2 does, however, guarantee that the only possible symmetry generated subgroups are those satisfying (2.2). In these instances we must use other techniques, such as Hopf bifurcation, to prove the existence of robust periodic solutions.

Acknowledgements. This work includes part of the Ph.D dissertation of PLB at the University of Houston. We thank Ian Stewart and Jim Collins for helpful discussions and comments. This research was supported in part by NSF Grant DMS-9704980 and Texas Advanced Research Program (003652037). We wish to thank the referees for several thoughtful and useful comments.

References

1. Alexander, R.McN.: Terrestrial locomotion. In: Mechanics and Energetics of Animal Locomotion, (R.McN. Alexander and J.M. Goldspink, eds), Chapman and Hall, London 168–203 (1977)
2. Blaszczyk, J., Dobrzecka, C.: Alteration in the pattern of locomotion following a partial movement restraint in puppies, Acta. Neuro. Exp., **49**, 39–46 (1989)
3. Barany, E., Dellnitz, M., Golubitsky, M.: Detecting the symmetry of attractors, Physica D, **67**, 66–87 (1993)
4. Buono, P-L.: A model of central pattern generators for quadruped locomotion, Ph.D Dissertation. University of Houston, August 1998
5. Buono, P-L.: Models of central pattern generators for quadruped locomotion. II. Secondary gaits, J. Math. Biol., **42**, 327–346 (2001)
6. Canavier, C., Butera, R., Dror, R., Baxter, D., Clark, J., Byrne, J.: Phase response characteristics of model neurons determine which patterns are expressed in a ring circuit model of gait generation, Biol. Cybern., **68**, 1–14 (1997)
7. Collins, J.J., Richmond, S.A.: Hard-wired central pattern generators for quadrupedal locomotion, Biol. Cybern., **71**, 375–385 (1994)
8. Cohen, A.H., Holmes, P.J., Rand, R.H.: The nature of the coupling between segmental oscillators of the lamprey spinal generator for locomotion: a mathematical model, J. Math. Biol., **13**, 345–369 (1982)
9. Collins, J.J., Stewart, I.: Coupled nonlinear oscillators and the symmetries of animal gaits, J. Nonlin. Sci., **3**, 349–392 (1993)
10. Crook, S., Cohen, A.: Central pattern generators. In: The Book of Genesis, (J.M. Bower and D. Beeman, eds.), Springer-Verlag, New York, 141–158 (1995)
11. Ermentrout, G.B., Kopell, N.: Multiple pulse interactions and averaging in systems of coupled neural oscillators, J. Math. Biol., **29**, 195–217 (1991)
12. Field, M., Melbourne, I., Nicol, M.: Symmetric attractors for diffeomorphisms and flows, Proc. Lond. Math. Soc., (3) **72**, 657–696 (1996)

13. Gambaryan, P.P.: How Mammals Run: Anatomical Adaptations, Wiley, New York (1974)
14. Golubitsky, M., Guillemin, V.: Stable Mappings and Their Singularities, Graduate Texts in Math. **14**, Springer-Verlag, New York (1973)
15. Golubitsky, M., Stewart, I., Buono, P-L., Collins, J.J.: A modular network for legged locomotion, Physica D, **115**, 56–72 (1998)
16. Golubitsky, M., Stewart, I., Buono, P-L., Collins, J.J.: The role of symmetry in animal locomotion, Nature, **401**, 693–695 (1999)
17. Golubitsky, M., Stewart, I., Schaeffer, D.: Singularities and Groups in Bifurcation Theory: II, Appl. Math. Sci., **69**, Springer-Verlag, New-York (1988)
18. Gray, J.: Animal Locomotion. Weidenfeld and Nicholson, London (1968)
19. Grillner, S.: Control of locomotion in bipeds, tetrapods and fish. In: Handbook of Physiology, Sect 1. The Nervous System, Vol. II. Motor Control (V.B. Brooks, ed.) American Physiological Society, Bethesda 1179–1236 (1981)
20. Grillner, S., Buchanan, J., Wallen, P., Brodin, L.: Neural Control of locomotion in lower vertebrates, In: Neural Control of Rhythmic Movements in Vertebrates (A.H. Cohen, S. Rossignol, and S. Grillner, eds.) New York, Wiley 129–166 (1988)
21. Hildebrand, M.: Analysis of the symmetrical gaits of tetrapods, Folia Biotheoretica, **VI**, 10–22 (1964)
22. Hildebrand, M.: Symmetrical gaits of horses, Science, **150**, 701–708 (1965)
23. Howell, A.B.: Speed in Animals. University of Chicago Press, Chicago (1944)
24. Kopell, N., Ermentrout, G.B.: Symmetry and phaselocking in chains of weakly coupled oscillators, Comm. Pure Appl. Math., **39**, 623–660 (1986)
25. Kopell, N., Ermentrout, G.B.: Coupled oscillators and the design of central pattern generators, Math. Biosci., **89**, 14–23 (1988)
26. Kopell, N.: Toward a theory of modelling central pattern generators. In: Neural Control of Rhythmic Movements in Vertebrates (A.H. Cohen, S. Rossignol, and S. Grillner, eds.) New York, Wiley 369–413 (1988)
27. Kopell, N., Ermentrout, G.B.: Phase transitions and other phenomena in chains of oscillators, SIAM J. Appl. Math., **50**, 1014–1052 (1990)
28. Kopell, N., Ermentrout, G.B., Williams, T.L.: On chains of oscillators forced at one end, SIAM J. Appl. Math., **51**, 1397–1417 (1991)
29. Melbourne, I., Dellnitz, M., Golubitsky, M.: The structure of symmetric attractors, Arch. Rational Mech. & Anal., **123**, 75–98 (1993)
30. Morris, C., Lecar, H.: Voltage oscillations in the barnacle giant muscle fiber, Biophysical J., **35**, 193–213 (1981)
31. Pearson, K.G.: Common principles of motor control in vertebrates and invertebrates, Annual Review of Neuroscience, **16**, 265–297 (1993)
32. Pribe, C., Grossberg, S., Cohen, M.A.: Neural control of interlimb oscillations II. Biped and quadruped gaits and bifurcations, Biol. Cybern., **77**, 141–152 (1997)
33. Rand, R.H., Cohen, A.H., Holmes, P.J.: Systems of coupled oscillators as models of central pattern generators, In: Neural Control of Rhythmic Movements in Vertebrates, (A.H. Cohen, S. Rossignol, and S. Grillner, eds.) New-York, Wiley 333–367 (1988)
34. Rinzel, J., Ermentrout, G.B.: Analysis of neural excitability and oscillations, In: Methods in Neuronal Modeling: From Synapses to Networks, (C. Koch and I. Segev, eds.), MIT Press, Cambridge, MA (1989)
35. Schöner, G., Jiang, W.Y., Kelso, J.A.S.: A synergetic theory of quadrupedal gaits and gait transitions, J. Theor. Biol., **142**, 359–391 (1990)
36. Williams, T.L., Sigvardt, K.A., Kopell, N., Ermentrout, G.B., Remler, M.P.: Forcing of coupled nonlinear oscillators: studies of intersegmental coordination in the lamprey locomotor central pattern generator, J. Neurophysiology, **64**, 862–871 (1990)